university of groningen

faculty of science and engineering

Impact of metabolic plasticity on microbial community diversity and stability

by

Thu Si Nguyen Mai | S4278836

supervised by

Sander G. van Doorn

Groningen, The Netherlands

July, 2021

Abstract

Microbial communities are crucial players in various biological systems. Their diversity and stability are usually associated with the health of organisms and the ecology and evolution of ecosystems. Although adaptive plasticity, specifically plasticity in metabolism, is ubiquitous in microorganisms, its impact on ecological properties of microbial communities remains elusive and understudied. Here, by utilizing metabolic networks reconstructed from the genomes of 18 human gut bacteria species and the dynamic flux balance analysis (dFBA), we modelled plastic metabolism in the studied bacteria and investigated its effect at both single species and community level. We showed that enabling metabolic plasticity has allowed many species to reach higher population densities at equilibrium in a variety of environments. Intrinsic plasticity was then measured as the capability of a species to exploit plasticity for its growth in a specific environment and was found to be determined both by the metabolic network of the species and its environmental condition. The results show that batch culture with fixed resources were less conducive to benefits from plasticity than continuous culture. Interestingly, variations in intrinsic plasticity among species were not correlated with their taxonomy. For small communities of two species, our simulations revealed that plasticity could foster competitive exclusion when the interacting species differed strongly in intrinsic plasticity. In those cases, the plastic species generally outcompeted the non-plastic one. Plasticity could also either hamper or facilitate competitive interactions. Importantly, we demonstrated that when there was plasticity, interaction coefficients inferred by fitting the generalized Lotka-Volterra (gLV) model to species densities data were incapable of reflecting species interactions at equilibrium. When the species were plastic, even if the inferred interaction coefficients were non-zero, most of the studied communities were likely to have little to no dependence between their members at equilibrium. These results also suggest that plasticity could promote stability by weakening ecological interactions. Nevertheless, several questions on the effect of plasticity on community stability remain after our analyses. First, new methods are needed to quantify the effect of plasticity on ecological interactions in a dynamic context; second, different measures have to be explored to track the propagation of perturbations through a community, and to quantify their impact. Future study therefore will have to address these remained issues and extend the research for a more thorough understanding of the impact of plasticity on species coexistence and dynamic interactions.

Keywords: adaptive plasticity, metabolic plasticity, microbial community, community diversity, community stability

Abbreviations

dFBA	Dynamic flux balance analysis
FBA	Flux balance analysis
gLV	Generalized Lotka-Volterra

Introduction

From human health to ecosystem functioning, microorganisms and their communities play crucial roles in a wide variety of biological systems at multiple ecological levels. At organism level, diversity and stability of microbiome has been linked to the health of plants [1], animals [2], and humans [3]. Microbial communities also have tremendous impact on the biodiversity and functions of ecosystems such as soils [4] and oceans [5]. Understanding microbial communities, therefore, is important, not only for deciphering mechanistically the behaviours of their associated biological systems but also for predicting and engineering those behaviours [3, 4, 6].

Recently, aided by the rapid advancement of sequencing technologies, there has been an escalating in descriptive findings on various microbial communities across space and time. Nevertheless, as increasingly detailed descriptions become available, there is also rising need for theoretical framework(s) that could help explain and generalize these descriptions in a both comprehensive and mechanistic manner [7, 8]. Indeed, although perhaps with a lower rate than that of empirical studies, there also has been an increase in theoretical and empirical-theoretical integrated studies in microbial community research. Most of them regarded the generalized Lotka-Volterra (gLV) model as a framework for the dynamics of the microbial communities being studied. The model has been utilized to study community network properties that link to diversity and stability of random and hypothetical communities [9], the assembly rules of the human gut microbiome [10–12], and the resilience of microbiomes to a wide range of perturbations – from antimicrobial treatment in the context of health [13] to climate change in the context of ecosystem management [14]. In a gLV model, a community is represented as a single matrix of intra- and inter-species interaction coefficients. On the one hand, this allows for generalizing the findings at a low computational cost, but on the other, it omits the extensive complexity in the interactions between microbial species which usually harbour a plethora of mechanisms and behaviours for interacting with their surroundings [15]. The gLV models also rely on the assumption of constant interactions between community members. Adaptive plasticity, however, is ubiquitous in microorganisms [16–18], and therefore, the assumption may be violated in many microbial systems in natural settings.

Different models, therefore, have been proposed. Those include, but are not restricted to, models of consumers and resources, in which community members are allowed to interact dynamically with each other through their metabolism [19–21]. Oña *et al.* modelled their microbial communities by networks of species linked with each other via nodes of their metabolites. Their results supported that strong cooperative cross-feeding promoted the robustness of communities to major disturbance [21]. The finding therefore is contradictory to that from the study of Coyte *et al.*, which was based on the gLV model and suggested that strong cooperation could have destabilizing effect on community stability [9]. Under usual metabolite-mediated models, however, adaptive plasticity in metabolism is still absent. The role of plasticity on community indeed is understudied not only in microbial community research but also in other biological systems research area. Pacciani-Mori *et al.* have emphasized this and therefore, designed their study to incorporate metabolic plasticity into the classical MacArthur's consumer-resource model. Their findings suggested that plasticity could support species coexistence in competitive communities [20]. A

limitation of the study, however, is that all members were assumed to be plastic and there was no possibility for cross-feeding.

Herein, with attempts to overcome the limitations of the above approaches, we utilized a mechanistic approach in modelling bacterial metabolism and aimed to study the effect of adaptive plasticity in metabolism, or shortly metabolic plasticity, both on the population growth at single species level and on the diversity and stability of microbial communities. Our approach involved metabolic networks reconstructed from the genomes of 18 human gut bacteria species and the dynamic flux balance analysis (dFBA) to model bacterial metabolism and to allow species to switch their metabolic strategies adaptively. *In silico* comparisons were conducted between when plasticity was permitted and when it was prohibited. At single species level, species were *in silico* cultured separately (mono-culture simulations), and their intrinsic plasticity were assessed as their capability to exploit plasticity for their growth. Intrinsic plasticity was examined not only across multiple species but also across differing environmental conditions, specifically differing media and culture types (batch and continuous culture). At community level, 10 representative two-member communities were studied in two representative media using dynamics simulations of co-cultures. Plasticity was assessed for its effects on species coexistence, species interactions, and community stability.

Methods

Genome-scale metabolic networks and media

We collected genome-scale metabolic networks and nutrient profiles of culture media from the AGORA database v1.3 [22]. These metabolic networks were reconstructed from bacterial genome sequences and refined with literature-derived experimental data. Differing media are defined based on various human diets and are described in details at https://www.vmh.life/. All 11 media available on the database were included in our study. However, the number of bacteria species were restricted to 18 species in total. The selection criteria were only to obtain a set of species from diverse taxonomy and whose growth were successfully calibrated by our simulations, as described below. List of selected species were provided in Table S1.

Dynamic flux balance analysis (dFBA)

When there is no metabolic plasticity (plasticity=OFF), a population was allowed to search for an optimal metabolic fluxes profile, i.e. metabolic strategy, corresponding to its initial environment. However, although the population growth and nutrient concentrations in the environment were constantly updated, the whole population would only follow its initial strategy for the entire course of the simulation, up to reaching equilibrium (stationary phase in batch culture simulations, but herein the two terms are used interchangeably). Standard flux balance analysis, therefore, was applied for the optimization problem, but only at the beginning of the simulations. Details of the flux balance analysis on metabolic networks are described elsewhere [22].

Dynamic flux balance analysis (dFBA) was applied when plasticity is allowed (plasticity=ON). In this scenario, the population was permitted to continually search for optimal metabolic strategy corresponding to its current environment. Each newly found metabolic strategy was introduced as a subpopulation. At every time step, it was possible for the population to harbour a maximum of 20 subpopulations. Switching therefore occurred as changes in density frequency between the subpopulations, with pre-defined constant switching rate (=3.5 h^{-1}), switching sensitivity of differences in growth rate between metabolic strategies (=0.05 h^{-1}), and a random effect.

The FBA estimates optimal metabolic fluxes profile by computing and optimizing the biomass production rate. Thus, to estimate the outcome of each optimal metabolic strategy found by FBA on the population growth, it is required to convert the associated biomass production rate into a growth rate. We involved two scaling parameters for this conversion: FLX representing how much resources or biomass a cell needs for growth and YLD representing the degrees of metabolic fluxes required for reaching a certain population density at equilibrium. The growth rate derived from this scaling was regarded as a sum of both the rate for cell maintenance (fluxNGAM) and the rate for cell replication. For all simulations, the fluxNGAM was constant and was 0.1 h^{-1}. FLX and YLD scaling parameters were estimated by fitting data after the initial FBA update to a reference growth curve with maximum growth rate and maximum density at equilibrium. Data from initial FBA was used in this calibration step because resources in initial environment are abundant and

therefore, initial growth rate was considered maximal. In principle, reference growth curves can come from empirical studies. However, as such empirical data were not available at the time the study was conducted, Monod's equations for growth under a limited resource were applied:

$\frac{dX}{dt} = X \cdot r \cdot \frac{S}{S+K_s}$ and $\frac{dS}{dt} = -X \cdot r \cdot \frac{S}{S+K_s} \cdot \frac{1}{Y} = -X \cdot \frac{S}{S+K_s}$, where S is resource concentration, X is population density, K_s =0.1 M is half-saturation constant, $r = \frac{\log(2.0)}{0.5}$ h^{-1} is maximum growth rate corresponding to generation time of 0.5 h under optimal growth condition, and $Y = r = 2\log(2.0)$ OD M^{-1} is yield coefficient. The initial population density was 1.0e-3 OD and initial resource concentration was 1.0 M.

Various characteristics of the systems can be monitored with our models. These include, but not restricted to, population growth rate and density, metabolic profiles of the population (fluxes of the metabolic network, resources consumption and production fluxes), and also the nutrient dynamics of the environment.

In silico culture

Simulations were implemented in C++11, supported with GNU Linear Programming Kit v5.0-1 (GLPK, http://www.gnu.org/software/glpk/), library LibSBML v5.19.0 [23], and Java environment v1.8.0_192.

Mono-culture simulations were conducted to study the effect of plasticity at single species level. Each of 18 selected species were *in silico* cultured independently in 11 differing media under either batch or continuous culture condition. Resources in batch culture were fixed. Meanwhile, the condition of continuous culture mirrored that in a chemostat, with the medium was continuously refreshed and bacteria were also washed out at a pre-define constant rate of 0.1 h^{-1}. Simulations with plasticity=OFF in principle are deterministic, but were still replicated 3 times. On the other hand, every species-environment case with plasticity=ON was replicated 10 times, due to the random effect in the modelled metabolic switching. In all simulations, initial population density was 1.0e-3 OD.

The effect of plasticity was next studied at community level with two-member communities. Within the scope of the project, the number of tested communities was narrowed to 10 and there were only two media selected for studying (*EU_avg* and *high_fat*). The communities were all possible pairs from a set of 5 representative species. The selection process was only based on the intrinsic plasticity (see below) across species and environments, but not on the resource consumption and production profiles. The study also focused on continuous culture experiments. Results from continuous culture experiments were expected to be more interpretable and biologically relevant. They showed more consistency between replicates (Fig. S1, S2, S4, and S5). More importantly, they allowed assessing competitive exclusion and the culturing condition also resembles more natural environments, such as one in the human gut. The number of replicates for each scenario of plasticity allowance was similar as in mono-culture experiments. All community species members also started with initial density of 1.0e-3 OD.

As previously mentioned, calibration was required in prior to culturing. Under the assumption

that all members in communities are equivalent in the extents of metabolic and biomass production rates required for maximal growth, a same set of FLX and YLD scaling parameters was used for all studied species. Species were first calibrated separately in differing media, then the maximum FLX value among all the cases and its associated YLD value was selected for all culture simulations. This was to enable the expected lowest growing population to fit the reference growth curve and to allow growth differences between species to be reflected in differences in their biomass production rate.

The final time point for the simulations was selected such that most of the growth curves reached stationary phase at the end of the simulation time interval. The simulation time for batch culture, in both mono-culture and co-culture, was 12.0 hours. For continuous culture, it was 144.0 hours in mono-culture and 96.0 hours in co-culture. These also enabled the estimation of species density at equilibrium as the density measured at the end of simulation. The notation for this variable was ρ, with ρ_{ON} and ρ_{OFF} denoted its value when plasticity=ON and when plasticity=OFF, respectively.

Effect of plasticity on species growth

The effect of plasticity on population growth of a species was measured as

$P = \frac{\rho_{ON}}{\rho_{OFF}}$.

In mono-culture, it was named as intrinsic plasticity (P_{mono}) and represented the capability of a species to exploit plasticity for increasing its population density at equilibrium ρ. In co-culture, P computed for every species member was denoted as P_{co}.

Classification of media and species

Differing media were hierarchical clustered based on their nutrient concentration profiles and on their species-wide intrinsic plasticity profiles under each culture type (batch or continuous). Nutrient diversity (H) was also computed using Shannon diversity index as follows

$H = \sum_{i}^{s} p_i \cdot \log_2 p_i$, where s is the total number of metabolites and p_i is the proportion of metabolite i in the medium.

Similarly, species were also hierarchical clustered based on their media-wide intrinsic plasticity profiles. All hierarchical clusterings were performed using euclidean distance and Nearest Point Algorithm.

Metabolite consumption-production profile

The dynamics of metabolite consumption and production of each population in mono-culture were extracted from the simulations and preprocessed. Specifically, fluxes for each metabolite were normalized by the total consumption or production fluxes at the corresponding time point. A metabolic consumption-production profile at a specific time point, hence, represented how much

each metabolite was consumed or produced with respect to the total consumption or production of the population.

Species coexistence

Species coexistence in co-culture experiments was regarded as the absence of competitive exclusion. In each simulation, a competitive exclusion event was indicated if one of the community member had ρ<0.01 OD. For a community, competitive exclusion then was quantified as the proportion of replicates indicated with competitive exclusion events and took positive value for the superior member and negative value for the inferior one.

Species interaction coefficients and linear stability analysis

In replicates where there were no competitive exclusion detected, species interaction coefficients were inferred. The inference involved the fitting of simulation data to the gLV model. Equation for the gLV model of a two-member community is as follows

$\frac{dX_i}{dt} = X_i(r_i + \alpha_{ii}X_i + \alpha_{ij}X_j)$, where X_i and r_i are respectively population density and intrinsic growth rate of species i; α_{ii} is intra-species interaction and α_{ij} is inter-species interaction indicating the effect of species j on species i. As intrinsic growth rate of a species is regarded as its growth rate when there is neither inter-species nor intra-species interactions, this was considered equivalent to species growth rate estimated at the beginning of our simulations, where population densities were still tiny and resources were abundant. To derive the intra- and inter-species interaction coefficients, ρ values in mono-culture and in co-culture were also used for fitting. Equations for the coefficients were, therefore,

$\alpha_{ii} = \frac{-1}{\rho_i} \cdot r_i$ and $\alpha_{ij} = (\frac{\rho_{i,ij}}{\rho_i} - 1) \cdot \frac{1}{\rho_{j,ij}} \cdot r_i$, where ρ_i is ρ value of species i in its mono-culture; $\rho_{i,ij}$ and $\rho_{j,ij}$ are respectively ρ values of species i and species j in their co-culture.

Linear stability analysis was subsequently performed on the fitted gLV models to infer the asymptotic stability of communities. The Jacobian matrix of the models were derived first, then a community was considered asymptotically stable if the largest real part among all eigenvalues of its associated Jacobian matrix ($\mathrm{Re}(\lambda)_{max}$) was below zero. In addition, the absolute magnitude of this $\mathrm{Re}(\lambda)_{max}$ was taken to be indicative of how quickly a stable community could return to its equilibrium [24].

Species persistence

Communities were also assessed for their species persistence upon perturbation. In each simulation, a pulse perturbation was introduced at 96.0 h time point, where most of simulations have reached equilibrium, and lasted for 1 hour. The perturbation introduced an 80% death rate to the perturbed population and was only applied to one of the community members per simulation. Species persistence was indicated as the ability of the perturbed species to recover and remain in the

community despite the perturbation.

Data visualization

All post-simulation data analyses were executed by scripting in Bash and Python v3.6.6 with Numpy v1.19.5 [25] and SciPy v1.5.4 [26]. Visualization of the results were also generated using Python v3.6.6 with libraries Matplotlib v3.3.4 and Seaborn v0.11.1 [27].

Results

Metabolic plasticity could support species growth

The effect of metabolic plasticity was first studied on every single species when they are grown in mono-culture and under differing environmental conditions – batch or continuous culture and multiple media with varying nutrient concentrations. An overview of the population density at ~equilibrium (ρ) across experimental settings indicates that adaptive plasticity could support bacteria reaching higher ρ ($\rho_{ON} > \rho_{OFF}$, i.e. ρ when plasticity is allowed (plasticity=ON) > ρ when plasticity is prohibited (plasticity=OFF), positive effect). Inherently due to the stochastic effect in the modelled metabolic switching behaviour, there were variations in ρ_{ON} and thus, variations in the effect of plasticity among replicates (Fig. 1A-B, S1, and S2). We discussed this further in the following section. Nonetheless, despite the variations, the effect of plasticity was only either positive or neutral ($\rho_{ON} \geq \rho_{OFF}$), confirming that the modelled metabolic plasticity was adaptive (Fig. 1A-B, S1, and S2). We were also able to demonstrate the effect of plasticity mechanistically, by examining the dynamics of population growth rates and metabolic activities monitored by our simulations. The curves of growth rate over density display diauxic shifts in cases with positive effect of plasticity. On the other hand, when the effect was neutral or when plasticity was disabled, there was no diauxic shift observed (Fig. 1A-C). Additionally, the occurrences of diauxic shifts were also associated with changes in metabolite consumption-production profiles of the populations (Fig. 1).

A positive effect of plasticity represents the significance of plasticity in the growth of a species in a certain environment. It also implies that the species was capable of exploiting plasticity to consume resources efficiently and enlarge its population under such an environmental condition. A neutral effect, on the other hand, reflects that plasticity was not exploited and played no significant role in the species growth. We therefore translated the effect of plasticity in mono-culture into a proxy for the intrinsic plasticity of a species in a specific environment (P_{mono} , see Methods). Generally, the more positive the effect, the greater the intrinsic plasticity a species is considered to have in the corresponding environment. Our overall result in mono-culture is that intrinsic plasticity was highly dependent on culturing type, which in this case is either batch or continuous culture. Moreover, it was also dictated by the interplay between the medium and the metabolic network of the species. More details of these results are reported in the two below sections.

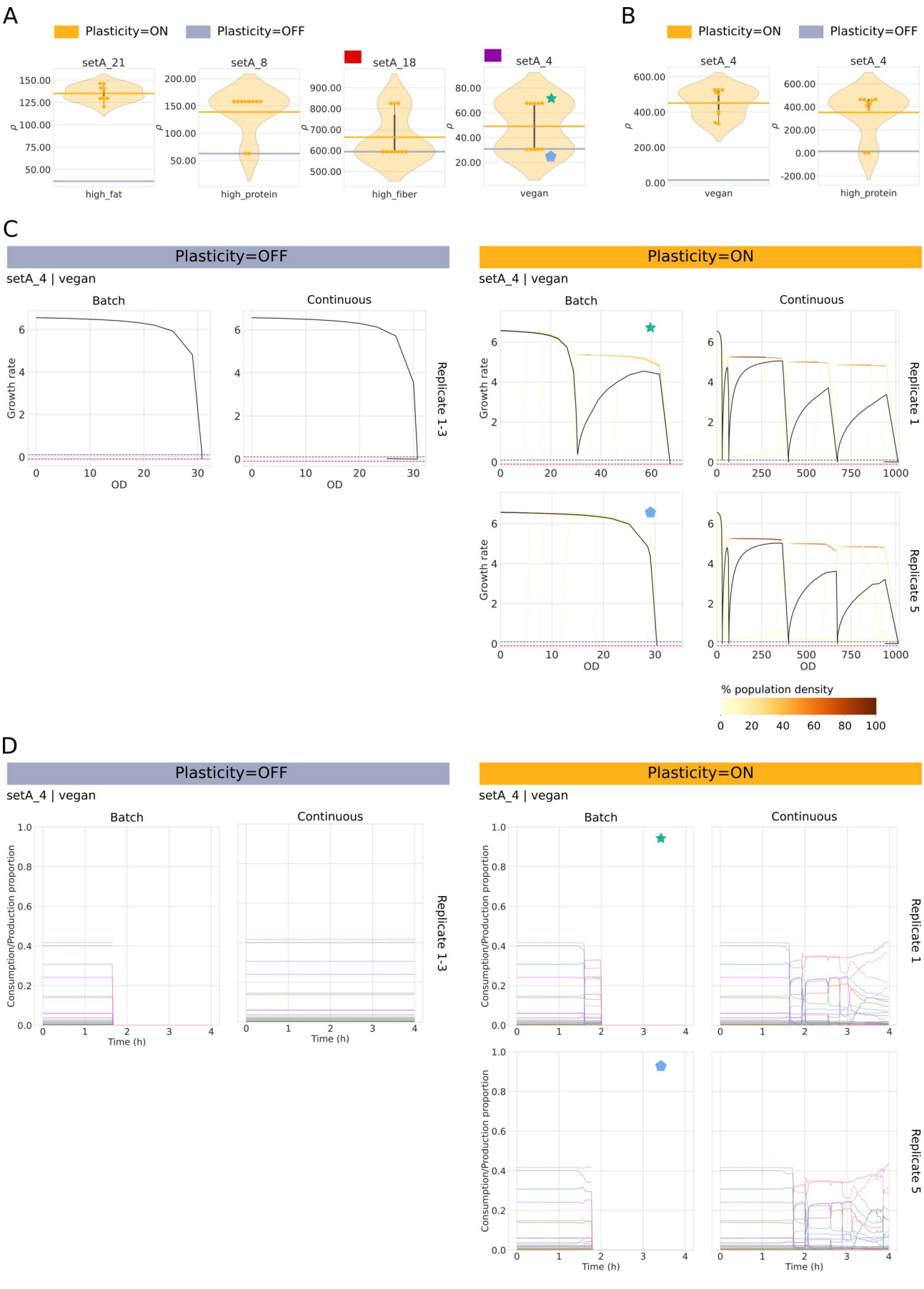
A
Plasticity=ON
Plasticity=OFF
setA_21
setA_8
setA_18
setA_4
high_fat
high_protein
high_fiber
vegan
B
Plasticity=ON
Plasticity=OFF
setA_4
setA_4
vegan
high_protein
C
Plasticity=OFF
Plasticity=ON
setA_4 | vegan
setA_4 | vegan
Batch
Continuous
Batch
Continuous
Growth rate
OD
Replicate 1-3
Replicate 1
Replicate 5
% population density
D
Plasticity=OFF
Plasticity=ON
setA_4 | vegan
setA_4 | vegan
Batch
Continuous
Batch
Continuous
Consumption/Production proportion
Time (h)
Replicate 1-3
Replicate 1
Replicate 5

Figure 1: Species growth with and without plasticity allowed. (A-B) Population densities at equilibrium (ρ, measured by densities the end of simulations – see Methods) of a few representative species-medium cases in batch and continuous mono-culture respectively. Yellow points and violin plots illustrate the distributions of multiple densities ρ_{ON} (ρ when plasticity=ON) resulted from 10 replicates. Yellow horizontal lines represent the means of ρ_{ON}. Greyish blue lines represent ρ_{OFF} (ρ when plasticity=OFF), which have no stochasticity and take single value for each species-environment case. In (A), the red box denotes a representative case with majority of replicates having $\rho_{ON} \approx \rho_{OFF}$ and ≤3/10 total replicates having $\rho_{ON} > \rho_{OFF}$, while the purple box denotes a representative case with bimodal distribution of ρ_{ON}. (C) Curves of growth rate over density (OD) of *setA_4* in *vegan* medium when plasticity=OFF (left panel) and plasticity=ON (right panel). Illustrated data were from the first 4 hours of the simulations. Black bold lines display the average values for the entire populations. When plasticity=ON, proportions of populations that had values differing from the population average values are represented by lines in yellow-orange-brown colour gradient (see Key). (D) Metabolite consumption-production profiles of *setA_4* in *vegan* medium when plasticity=OFF (left panel) and plasticity=ON (right panel). Illustrated data were from the first 4 hours of the simulations. For each metabolite, the consumption or production rate is from the entire population and was normalized by the total consumption or production rate. Consumed and produced metabolites are represented by bold and dashed lines, respectively. In (A, C-D), green stars and blue pentagons indicate two different replicates of *setA_4* in *vegan* medium and batch culture when plasticity=ON. The former indicate a single simulation in which $\rho_{ON} > \rho_{OFF}$, while the latter indicate a different single simulation in which $\rho_{ON} = \rho_{OFF}$.

Environments with fixed resources were unfavourable for plasticity

We predicted that batch culture could be less conducive to benefits from plasticity than continuous culture. These culture types provide two differing regimes governing how resources are provided and how the bacteria are retained in the environment. Batch culture is a closed system in which all resources are provided once and fixed and all the bacteria, either dead or alive, permanently stay within the environment. Continuous culture, in contrast, is an open system with resources continuously refreshed and bacteria washed out at a constant rate. As a consequence, the efficiency of exploiting plasticity required to achieve a higher ρ_{ON} (than ρ_{OFF}) in batch culture could be higher than that in continuous culture. In other words, it could be more difficult for the bacteria to benefit from plasticity in batch culture, unless they are very efficient in exploiting it. Therefore, it was expected that positive intrinsic plasticity could be found less frequently and with lower values in batch culture.

We indeed observed outcomes consistent with our expectation in the results across various experimental settings. For most of the combinations of species and media, intrinsic plasticity in continuous culture was found to be higher than that in batch culture (Fig. 2). Additionally, in several cases of batch culture, a high value of intrinsic plasticity was also unrepresentative, owing to the large inconsistencies among replicates (Fig. 1A and 2, cases annotated with red and purple boxes; Fig. S1). In these instances, the majority of replicates showed ~zero intrinsic plasticity ($\rho_{ON} \approx \rho_{OFF}$) and only very few replicates with intrinsic plasticity ($\rho_{ON} > \rho_{OFF}$, at most 3/10 total replicates) (Fig. 1A and 2, cases annotated with red boxes; Fig. S1). The distribution of ρ_{ON} was also sometimes bimodal or approximately bimodal, and in the latter cases, replicates with ~zero intrinsic plasticity still took up a higher proportion (Fig. 1A and 2, cases annotated with purple boxes; Fig. S1). Conversely, in continuous culture, replicates with intrinsic plasticity were always

the majority (at least 8/10 total replicates) (Fig. 1B and S2). Inconsistencies among replicates arose from variations in ρ_{ON}, which inherently stemmed from the random effect added to the decision making of bacteria in metabolic switching. Our results, therefore, suggest that switching to the right strategy at the right moment could be more critical in environments with fixed limited resources. Indeed, a more mechanistic view into the growth rate and metabolism dynamics show that it was more frequent in batch culture that diauxic shift could not take place before the resources ran out and the population stopped growing, resulting in more replicates with zero intrinsic plasticity (Fig. 1).

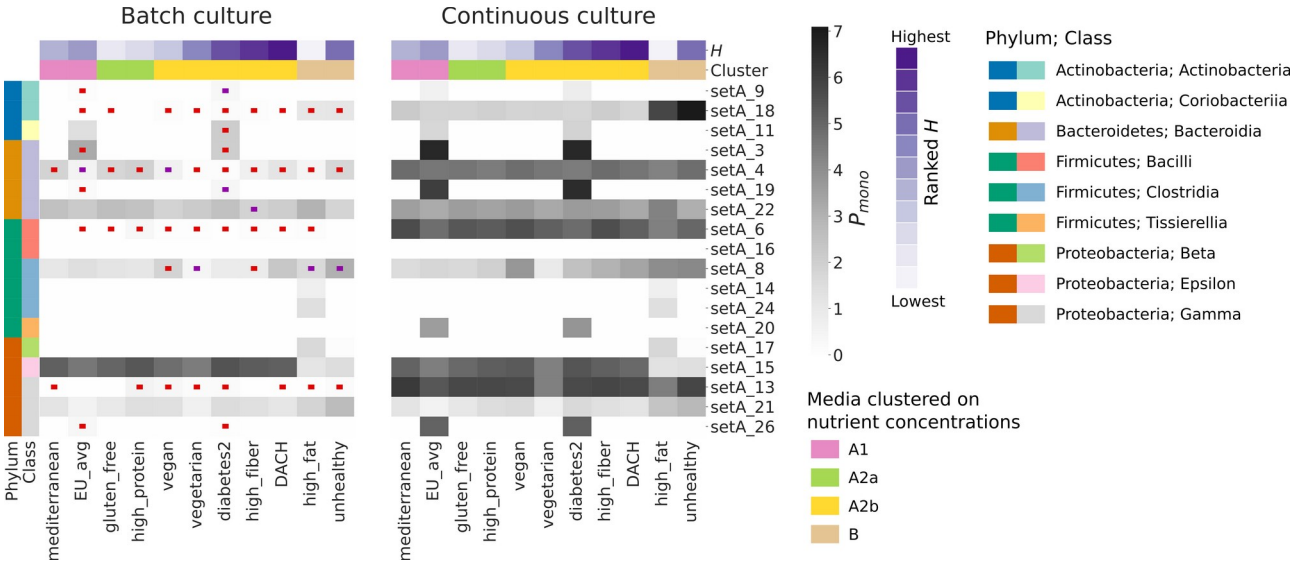

Figure 2: Intrinsic plasticity across species and environmental conditions. The heatmaps illustrate intrinsic plasticity values (P_{mono}) across all studied species (n=18) in all tested media (n=11) in batch (left) and continuous (right) culture. Species are annotated for their taxonomy at phylum and class levels by the two leftmost columns (see Key). By the two uppermost rows, media are, sequentially, annotated for their ranked Shannon nutrient diversity (H, see Key) and their associated principal clusters resulted from hierarchical clustering on nutrient concentration profiles (see Key and Fig. 3). In the heatmap of batch culture results, red boxes denote cases with majority of replicates having $\rho_{ON} \approx \rho_{OFF}$ and ≤3/10 total replicates having $\rho_{ON} > \rho_{OFF}$, while purple boxes denote cases with bimodal or approximately bimodal distributions of ρ_{ON} (see Fig. 1A, S1, and S2 for clarification).

Both species and environmental conditions determined intrinsic plasticity

Intrinsic plasticity in general was determined by the interplay between metabolic networks of species and environmental conditions.

Firstly, how unfavourable the batch culture is for exploiting plasticity was variable across both differing species and differing media. Some species were able to have high intrinsic plasticity regardless of the culturing type (e.g. *setA_15*) while others were not and their intrinsic plasticity was dramatically hampered in batch culture (e.g. *setA_13*) (Fig. 1A). Intrinsic plasticity of a species could also be affected by culturing type to a greater extent in a medium but to a lesser extent in the other one. For example, batch culture was more unfavourable for plasticity of *setA_22* in *high_fiber*

medium than in *vegetarian* medium. Intrinsic plasticity of the species was lower in batch than in continuous culture if *high_fiber* medium was supplemented, but with *vegetarian* medium, the difference between the two culturing types was not significant (Fig. 2, S1, and S2).

Furthermore, under a same culturing type, nearly all species displayed varied intrinsic plasticity across tested media. Specifically, a species could have very high intrinsic plasticity in one medium but have almost no intrinsic plasticity in the other medium (Fig. 2). However, intrinsic plasticity could be similar between some media with shared nutrient profiles, and media could be hierarchically clustered by their species-wide intrinsic plasticity profiles (Fig. 2, 3, and S3). For instance, it was found that species usually expressed similar intrinsic plasticity in *EU_avg* and in *diabetes2*. In addition, there were also more species found to have intrinsic plasticity in these two media than in other media, suggesting that they could be more favourable for plasticity (Fig. 2 and S3). The clustering of media based on intrinsic plasticity was also used to compare with the clustering based on nutrient concentrations (Fig. 3) and with the variations in Shannon nutrient diversity (H , see Methods). One notable finding from this is that *high_fat* and *unhealthy* shared similar profiles both in nutrients content and in intrinsic plasticity (Fig. 2, 3, and S3). The analyses also show that intrinsic plasticity clustering appeared to be more correlated with nutrient concentrations clustering than with variations in H (Fig. 2, 3, and S3), suggesting that intrinsic plasticity could be more dependent on the quota of certain essential nutrients than on the nutrient diversity of the medium.

How favourable a medium is for intrinsic plasticity, however, was not exhaustively general for all species. Intrinsic plasticity was also species-dependent and the variations in intrinsic plasticity between media were different among species. Some species showed nearly homogeneous medium-wide profiles. They expressed high intrinsic plasticity in almost all media (e.g. *setA_13*, *setA_4* in continuous culture) or no intrinsic plasticity at all in any environmental condition (*setA_16*). On the other hand, other species appeared to have preferential media where they expressed intrinsic plasticity exclusively or significantly higher (e.g. *setA_15*, *setA_24*) and their preferences were also diverse (Fig. 2). Nonetheless, similar to media, species can also be stratified by their intrinsic plasticity profiles, suggesting a statistical structure in the diversity among them (Fig. S3). Importantly, variations in intrinsic plasticity between species showed almost no correlation with species taxonomy at both phylum and class levels (Fig. S3). Species from differing phyla and/or classes could have similar intrinsic plasticity profiles (e.g. *setA_26* and *setA_19*), but the profiles of species from a same class could be considerably dissimilar from each other (*setA_6* and *setA_16*) (Fig. 2 and S3). These suggest that if metabolic interactions play a major role in the ecology of microbial communities, then it is probable that intrinsic plasticity could be a stronger predictor for the ecological function of a species than taxonomy classification.

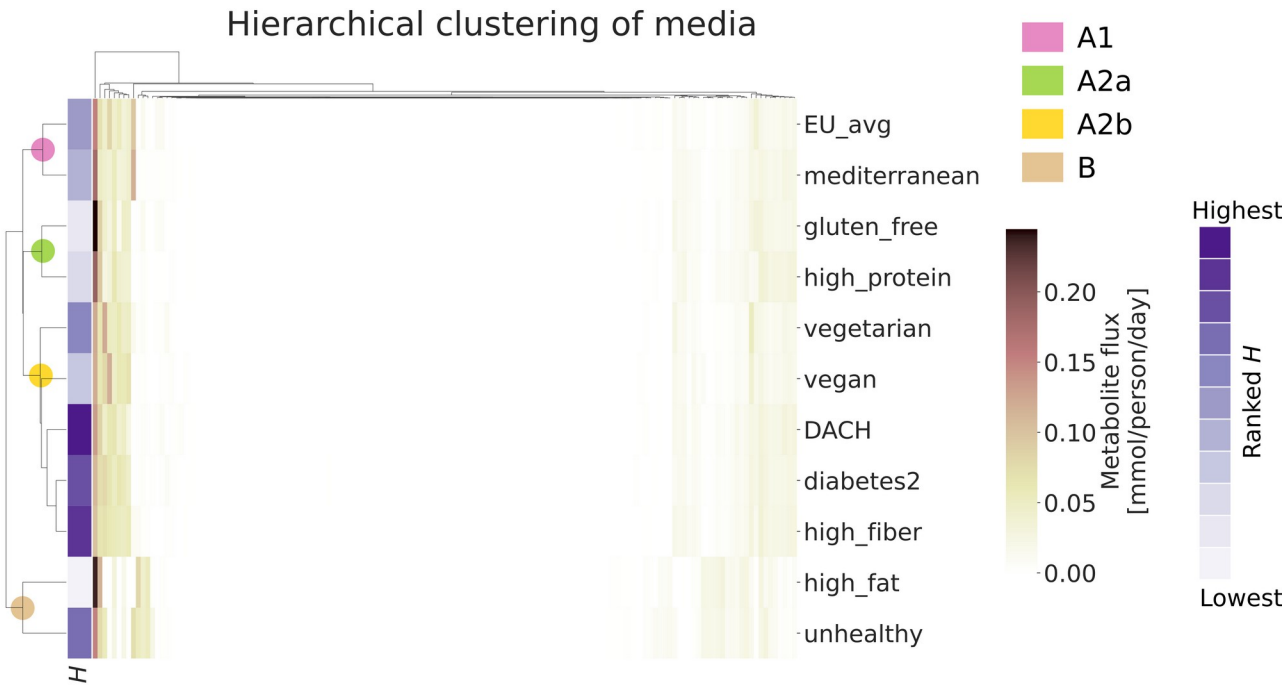

Figure 3: Classification of media. The left-hand vertical dendrogram displays the hierarchical clustering of 11 studied media based on their nutrient concentration profiles. The clustering resulted in 5 principal clusters: A1, A2a, A2b, and B, which are indicated by circles in differing colours at the corresponding nodes (see Key). The adjacent column indicates the ranked Shannon diversity (H , see Key) of the media, which were also based on their nutrient concentration profiles. These profiles are illustrated by the adjacent heatmap with rows corresponding to multiple metabolites. Each cell corresponds to the metabolite concentration (flux), measured in mmol/person/day based on the human diet type defining the associated media (see Key). Metabolites were also hierarchically clustered, by a similar method and represented by the top horizontal dendrogram.

Adaptive plasticity could strongly affect species coexistence and interactions

We next studied the effect of metabolic plasticity on species coexistence and interactions in 2-member communities. Due to the high computational cost of community simulations, our investigation was narrowed to a small subset of 10 communities comprising of 5 representative species and studied in environments supplemented with either *EU_avg* (average Western diet) or *high_fat* (high-fat and low-carb diet) medium. The species and media were selected such that diverse scenarios of variation in intrinsic plasticity between co-inhabitants and between media could be included. To avoid bias, we did not select species based on their metabolite consumption-production profiles. We also focused our analyses on continuous culture experiments, since competitive exclusion could not be inferred from those in batch culture. Results from continuous culture experiments were also expected to be more interpretable and biologically relevant as they showed more consistency between replicates (Fig. S1, S2, S4, and S5) and the culturing condition resembles more natural environments, such as one in the human gut.

Studying the effect of plasticity in co-culture, we first computed P_{co} for every species in each community using a similar formula for computing intrinsic plasticity P_{mono}. The values of P_{co}, therefore, are also proportional to how higher density a species could reach at ~equilibrium when

plasticity=ON compared to when plasticity=OFF. Examining P_{co} with respect to P_{mono}, we found that species which had intrinsic plasticity (in mono-culture) also expressed positive P_{co} and those which did not had intrinsic plasticity also showed ~zero P_{co} (Fig. S6). However, it is difficult to interpret from these results whether a positive P_{co} indicates that the species was able to retain their capability of utilizing plasticity or the species was positively affected by the co-inhabitant or the combination of both. This ambiguity in the meaning of P_{co} was exemplified by the strikingly negative values in species with no intrinsic plasticity (Fig. S6). Since our modelled plasticity was adaptive (as discussed above), it was revealed that P_{co} also encapsulates effects from species interactions, which in these cases could be negative.

The effect of plasticity, thus, was then assessed specifically on species coexistence (represented for community diversity, qualitative effect) and species interactions (quantitative effect) and separately on each case of plasticity allowance (plasticity=ON or plasticity=OFF). Species coexistence was represented by the absence of competitive exclusion. Competitive exclusion was measured as the proportion of replicates with almost only one species remained at the end of simulations. The values took positive sign for the superior co-inhabitant and negative sign for the inferior co-inhabitant. Where there was no competitive exclusion, species interaction coefficients were inferred by fitting the generalized Lotka-Volterra (gLV) model to species densities data from the simulations. For each species member in a community, the derived intra-species interaction coefficient was inversely proportional to its ρ in mono-culture and the inter-species interaction coefficient was proportional to the ratio of its ρ in co-culture over its ρ in mono-culture. As expected, the computation resulted in reduced intra-species interactions when plasticity=ON in species with intrinsic plasticity (Fig. S7C-D).

In both tested media, allowing plasticity led to more competitive exclusion. However, all competitive exclusion instances were only at communities with one or both members that did not expressed intrinsic plasticity. Communities underwent competitive exclusion when plasticity was prohibited were comprised of only the latter cases, in which allowing plasticity could not have any effect. Hence, we were not able to explore whether plasticity could obstruct competitive exclusion and facilitate coexistence. In the former cases, enabling plasticity led to competitive exclusion, which was not occurred when plasticity was disabled. Nonetheless, it should be noted that member that had intrinsic plasticity was always the superior (Fig. 4A-B and S7). Additionally, we found that inter-species interactions of these communities were mostly negative when plasticity=OFF (Fig. 4A-B and S7). These results, therefore, reveal that if plasticity was allowed but only one of the members was capable of utilizing it, inter-species competition could be dramatically intensified and competitive exclusion could be fostered.

Inter-species interaction coefficients when there was no plasticity were mostly neutral, but there was no positive instance found and a number of communities demonstrated either negative-neutral (-/0) or negative-negative (-/-) relationship. Many of the negative relationships corresponded to competitive exclusion when plasticity was introduced, as described above. However, we also recorded 2 cases in which (-/0) relationships changed into (0/0) following the introduction of plasticity and members that received the positive effects also had intrinsic plasticity.

For communities with neutral relationship (when plasticity=OFF), enabling plasticity also appeared to have both negative and positive impacts. There were cases corresponding to competitive exclusion, (-/0), or positive-neutral (+/0) when plasticity=ON. As can be seen, we did not obtain any cases in which the impact of plasticity led to mutually beneficial (+/+) nor mutually harmful (-/-) relationships, even when all the co-inhabitants possessed intrinsic plasticity. Moreover, not only species that were positively affected were those that had high intrinsic plasticity but also those that were negatively affected were the ones with higher intrinsic plasticity in the community (Fig. 4A-B and S7). Nevertheless, it could not be concluded from the computed coefficients whether or not cooperation or competition has been facilitated by plasticity. This is because the negative or positive effects observed from these results only expressed changes in the ratio of ρ in co-culture over ρ in mono-culture. They did not necessarily reflect changes in species interactions at equilibrium, particularly when plasticity was permitted and there were at least one co-inhabitant capable of utilizing it. When there was plasticity, the bacteria changed their metabolic behaviours and, therefore, both of their intra- and inter-species interactions very dynamically throughout the co-living period. Consequentially, co-inhabiting species could have been propelled by each other to the metabolic states (at equilibrium) that were different to where they were in mono-culture equilibria. Whether such new states led to higher, lower, or unchanged ρ resulted in respectively positive, negative, or neutral interaction coefficients (Fig. 5), but it was uncertain whether there were any forms of cooperative or competitive interactions at the new states. Notwithstanding these limitations, since the coefficients could still reflect species interactions when there was no plasticity, if a negative interaction coefficient was observed to be "neutralized" by plasticity (as in *setA_21* and *setA_11* in *EU_avg*, *setA_15* and *setA_24* in *EU_avg*, Fig. 4A-B), it is still likely that competitive interaction was avoided, thanks to plasticity.

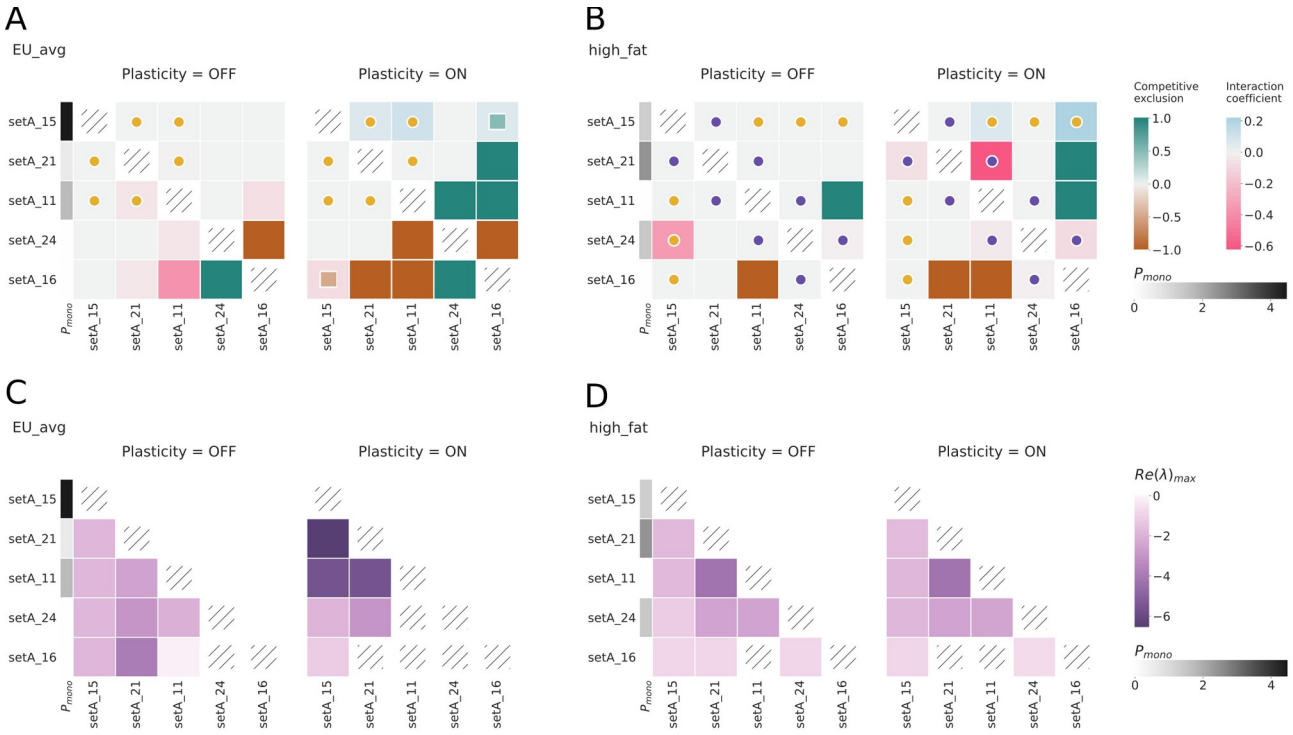

Figure 4: Inter-species interactions and linear stability of 2-member communities. (A-B) The heatmaps illustrate inter-species interaction coefficients overlaid with competitive exclusion measurements in continuous culture supplemented with *EU_avg* (A) and *high_fat* (B) media. Each

off-diagonal cell displays the value of species in the corresponding row when it was co-cultured with species in the corresponding column. For competitive exclusion measurements, positive values indicate the superior members while negative values indicate the inferior members. Their absolute values are the proportions of replicates with competitive exclusion events indicated (see Key). Interaction coefficients were inferred only if a simulation indicated to not experience a competitive exclusion event. The coefficient represented by an off-diagonal cell indicates the effect of species in the associated column on species in the associated row, which can be positive, negative, or neutral (+/-/0). At a community which was indicated with competitive exclusion in only a part of its replicates, competitive exclusion measurements are displayed by smaller squares, nested inside cells displaying species interaction coefficients. Yellow points indicate communities in which interaction coefficients were more positive when plasticity=ON than when plasticity=OFF, while dark purple points indicate communities with the opposite figures. (C-D) Community stabilities ($\mathrm{Re}(\lambda)_{max}$) measured by linear stability analyses in continuous culture supplemented with *EU_avg* (C) and *high_fat* (D) media. Stabilities were measured only in simulations without competitive exclusion indicated. In each (A), (B), (C), and (D), the leftmost column corresponds to the intrinsic plasticity (P_{mono}) values of the species.

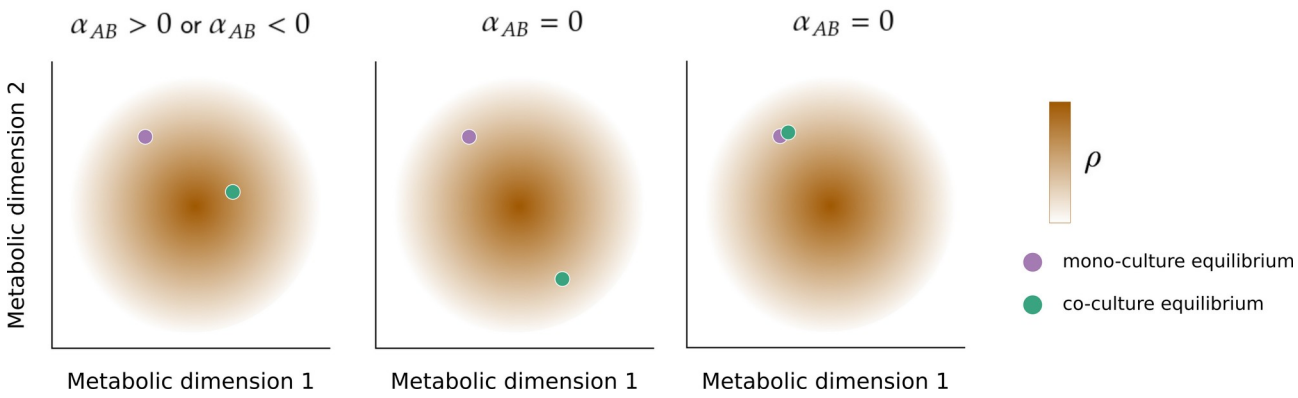

Figure 5: Association between changes in metabolic state and inter-species interaction coefficients when there is plasticity. The illustration depicts three possible scenarios of change in the metabolic state of a species at its co-culture equilibrium (green points) compared to that at its mono-culture equilibrium (violet points), when there is metabolic plasticity. The outcomes of those scenarios in the inter-species interaction coefficients (α_{AB}), inferred by fitting species density measurements at mono- and co-culture equilibria to a gLV model, are specified correspondingly. The metabolic space of the focal species is hypothesized to have or to have been scaled to 2 dimensions. The colour gradient of the space represents the gradient in population density of the species at equilibria (ρ). If darker shades correspond to higher ρ, then the leftmost scenario corresponds to α_{AB} >0, and vice versa. In the other two scenarios, both mono-culture and co-culture equilibria have equivalent ρ and thus, result in α_{AB} =0, regardless of the degree of difference in the metabolic states.

A first look at community stability

Following the inference of species interaction coefficients, community stability was first inferred via linear stability analyses on the gLV models fitted to our simulation outcomes (see Methods). Under this method, stability was measured as local asymptotic stability, indicating whether a community would return to its equilibrium following a transient change in the density of any of the species member at that equilibrium. A community would be asymptotically stable if the

largest real part among all eigenvalues of its gLV model's Jacobian matrix ($\mathrm{Re}(\lambda)_{max}$) was below zero. In addition, how quickly a stable community would return to its equilibrium was indicated by the absolute magnitude of this $\mathrm{Re}(\lambda)_{max}$.

When there was no plasticity, the community with (-/-) interactions (*setA_16* and *setA_11* in *EU_avg*) was the least stable one. However, there were no significant differences in stability between (-/0) and (0/0) communities (Fig. 4C-D). As plasticity being introduced, more than half of communities that experienced positive effects on interaction coefficients (changed from (-/0) to (0/0) or from (0/0) to (+/0)) showed increased stability (Fig. 4, communities annotated with yellow points). Meanwhile, at communities that experienced negative effects, the differences in stability between with and without plasticity were not significant (Fig. 4, communities annotated with dark purple points). These suggest that plasticity could support community's asymptotic stability around its equilibrium. However, this is only under the conditions that the inferred interaction coefficients have precisely reflected the interactions between species at equilibrium and that those interactions would be constant upon transient perturbations. As discussed above, such conditions might have been violated when there was plasticity.

As can be seen, when species were adaptively plastic in their metabolism, the results from applying the gLV model were seismically ambiguous to interpret. Therefore, to further investigate the impact of plasticity on community stability, we experimented with directly introducing perturbations into our dynamic flux balance analysis (dFBA) simulations. Perturbation was introduced after 96.0 hours of co-culture, when most of simulations had reached steady states, and then lasted for 1 hour (pulse perturbation). The perturbation induced an 80% death rate to the perturbed population, mimicking events such as bacteriophage lysis. In addition, to explore the persistence of each member in the community, there was only one member that was perturbed in each simulation, and thus, there were two experiment settings for each community.

The results show that regardless of the presence of plasticity, the introduced perturbations did not lead to any extinction and all of the species were able to retain their population during and after perturbation (Fig. 6, S8, and S9). Therefore, the effect of plasticity on species persistence was not observed. Nevertheless, the results reveal certain insights into the species interactions at equilibrium, which could not be interpreted from the interaction coefficients inferred from fitting the gLV model to species densities data. We observed that when there was no plasticity, there was usually a spike in population of the unperturbed member during perturbation if the community expressed a (-/0) or (-/-) relationship, indicating competitive interactions at equilibrium (the only exception was community of *setA_11* and *setA_24* in *EU_avg*). By contrast, when there was plasticity, the unperturbed member in most of the communities appeared to be not affected by the perturbation, suggesting that there could be little to no interaction between community members at the equilibrium, even when the interaction coefficients were not (0/0) (Fig. 4A-B, 6, S8, and S9). The findings here, therefore, support that when there was plasticity, species interactions at equilibrium in co-culture could not be thoroughly captured by the coefficients inferred from the fitted gLV models. In addition, for communities with positive or negative coefficients (when plasticity=ON), they also suggest that affected by both plasticity and co-living, species were propelled to metabolic states that gave rise to higher or lower ρ than in their mono-cultures (Fig. 5), but at equilibrium, their existence were not or nearly not affected by their co-inhabitants. As

there was likely no species interaction at equilibrium, it was also suggested that those communities could be asymptotically stable. Nevertheless, we did observed a community in which negative coefficients when plasticity=ON possibly were associated with competitive interactions. The community comprised *setA_24* and *setA_16*, cultured in *high_fat* medium. When plasticity=ON, their interaction coefficients were (-/-) and there was an elevation in *setA_16* population when the *setA_24* was perturbed. As their interaction coefficients when there was no plasticity were much less negative (-/0 but approximately 0/0), these findings suggest that plasticity has facilitated competition in this community (Fig. 4A-B, 6, S8, and S9).

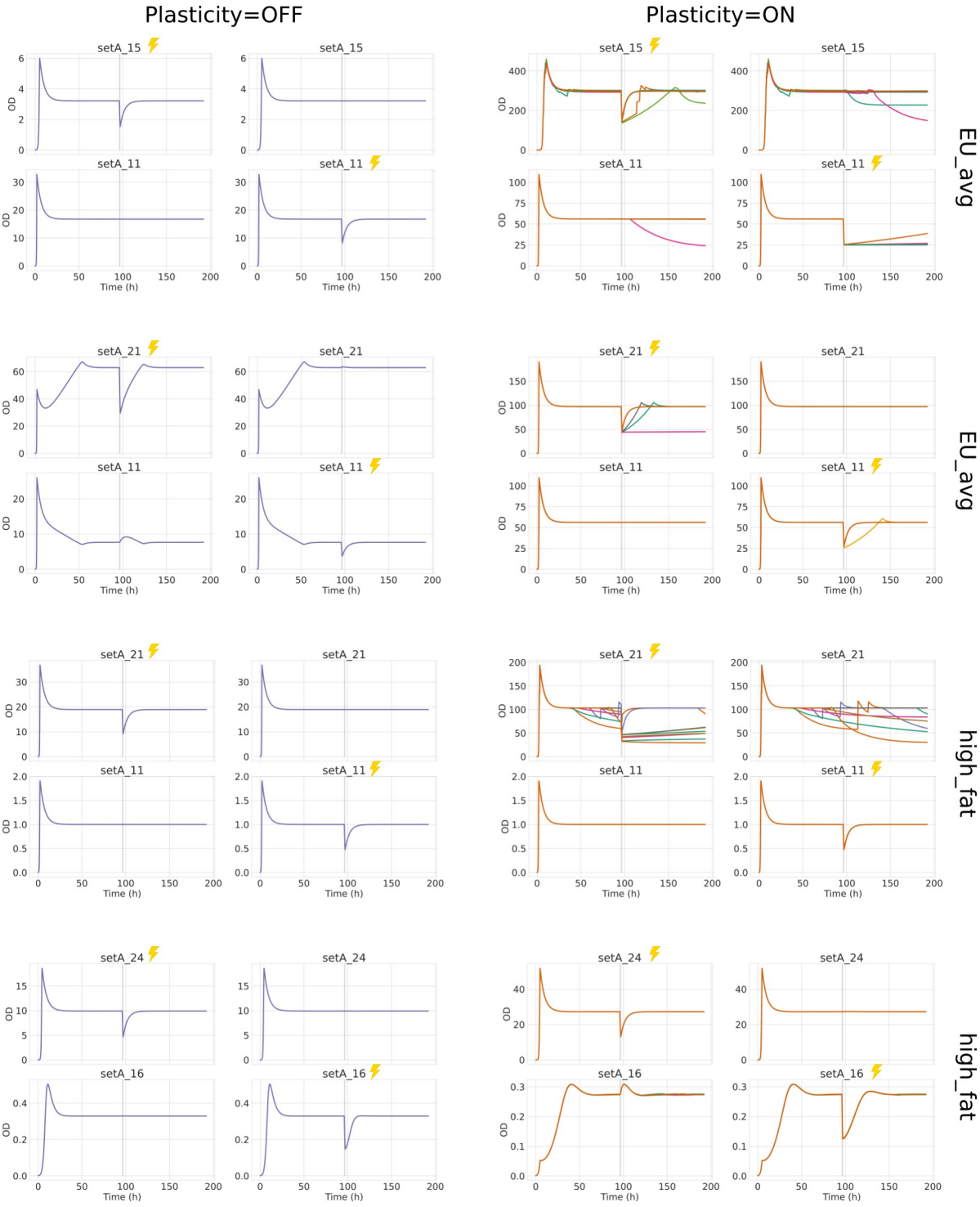

Figure 6: Species persistence upon perturbation. Plots of species density over time in co-culture simulations with pulse perturbations when plasticity=OFF (left panel) and when plasticity=ON (right panel) of 4 representative community-medium cases. Names of supplemented media are specified in the right border of the figure. Thin vertical blocks in grey highlight the period that the perturbations occurred (duration of 1 hour). Yellow lightning bolts indicate species members which the introduced perturbations targeted to. When plasticity=ON, multiple curves in different colours represent results from different 10 replicates.

Discussion

Utilizing dFBA with genome-scale metabolic models of 18 gut bacteria species, we were able explore the impact of adaptive plasticity both on species growth in mono-culture and on species metabolic interactions in microbial communities. This mechanistic approach has enabled us avoid the assumptions of constant species interactions of the gLV model as well as the bias accompanying with pre-defined species metabolism. The bacteria were allowed to find and switch to the metabolic strategy that is optimal for their growth rate during their living and therefore, to interact dynamically with their environment and with other co-inhabitants. Furthermore, although the metabolic networks were pre-defined, the experiments were still blind to their metabolic spaces in differing environments, enabling us to discover unexpected behaviours. The use of metabolic networks reconstructed from bacteria genomes also allowed us have biologically relevant constraints on the metabolic spaces that are specific to each different species.

As expected, the allowance of plasticity has facilitated the growth of many species in a variety of environments, resulting in their elevated population densities at equilibrium. However, the extent to which a population could exploit plasticity for its growth, measured by intrinsic plasticity, was variable among differing species and environmental conditions. We observed that batch culture conditions, with fixed limited resources, were more unfavourable for intrinsic plasticity than continuous culture conditions, in which resources were continuously refreshed. Furthermore, intrinsic plasticity was also determined by the interplay between species and supplemented media. Intrinsic plasticity of species appeared to be dependent more on nutrient abundance than on nutrient diversity of the media. More notably, species intrinsic plasticity was not correlated with species taxonomy, suggesting that intrinsic plasticity could be a better predictor for the ecological function of a species. This, however, is under the condition that the ecological function of a species is mainly defined by its metabolism. Herein, a species was represented only by its metabolic network. Certainly, bacteria have a plethora of behaviours that could also be important for their ecological role, such as toxin production [28] or motility and chemotaxis [29, 30]. Although there are limitations in bridging our results to natural biological systems, there could be avenues in studying bacterial metabolic networks. One possibility for extending research could be exploring network properties that are associated with plasticity behaviours. Also, it should be noted that intrinsic plasticity was only measured as the outcome of plasticity in final population density. This proxy did not imply about the metabolic switching behaviours of the species, i.e. the metabolic networks, which could be, for instance, the frequency and amplitude of metabolic switching.

The work of Pacciani-Mori *et al.* showed that allowing adaptive switching, i.e. plasticity, of metabolic strategies promoted species coexistence in competitive communities. However, in their model, when plasticity was introduced, all community members were assumed to be plastic [20]. As described above, this might not be the case for metabolic plasticity in bacteria. When two co-inhabitants differed strikingly in intrinsic plasticity, we found that plasticity could intensify competition and foster competitive exclusion. In such cases, it appeared that plasticity has allowed the plastic member to be much more metabolically efficient (for its own growth) such that it outcompeted the other non-plastic member, whose metabolic strategy was fixed and probably much less efficient. We were not able to study if plasticity could also instead foster species coexistence

and hamper competitive exclusion, since all competitive exclusion events when there was no plasticity were only observed in communities with non-plastic members. Nonetheless, findings from studying species interactions and species persistence show that plasticity could help species avoid competition. Species interaction coefficients were inferred by integrating mono-culture and co-culture densities at equilibria into the gLV model, and experiments for species persistence involved the introduction of a pulse perturbation onto one of the community members after the community has reached equilibrium. From the results, we have identified two communities in both two tested media, whose interaction coefficient pair was (-/0) when there was no plasticity, but was (0/0) when plasticity was present. Additionally, in these communities, when they were not plastic, perturbing one member after the community has reached equilibrium resulted in a spike in the population of the other, but when they were plastic, community members appeared to be not affected by the perturbation at their co-inhabitants. However, we also recorded one community showing a completely opposite figure. Their interaction coefficients were significantly more negative as plasticity was introduced and perturbing one of the members was associated with a spike in density of the other, which mirrored figures of other competitive communities when there was no plasticity. Hence, it appeared that allowing species to explore and switch their resource consumption strategies, could either prevent or facilitate competition, probably depending on whether the optimal strategies lie within the niche overlaps.

Except from the above community, most of other communities which showed a transition from (0/0) coefficients when plasticity=OFF to (-/0) or (+/0) coefficients when plasticity=ON did not display any dependence upon perturbation. These demonstrate that when there is adaptive plasticity, interaction coefficients inferred by fitting the gLV model could falsely capture interactions at equilibrium between community members, due to the violation of the gLV model's assumption on constant interaction. In our case of metabolic interactions, plastic community members could have interacted very dynamically such that they were propelled by each other to metabolic states that were different from ones in their mono-cultures. As illustrated in Fig. 2E, such new states might result in higher, lower, or unchanged densities compared to mono-culture densities, but they did not reflect the interactions between the members at their co-culture equilibria. Moreover, these could also be extended to the misinterpretation of species interactions from differences in species density or abundance observed over time. Whereas adaptive plasticity is ubiquitous in bacteria [16–18], it has been a common practice in microbial community research to infer about the communities' equilibria and dynamics by fitting population densities from empirical measurements into gLV models [12, 13, 31–33]. Our findings point to the shortcoming of this common approach and support the utilization and development of mechanistic techniques for directly measuring molecular interactions in microbial communities. Indeed, although to some extent, we were able to have a better look at species interactions by introducing perturbation to one of the community members, interpretations from these experiments are still limited. It is uncertain if the introduced perturbation was strong and prolonged enough to observe the dependence between community members. More importantly, it is also possible that owing to plasticity, species were able to become independent when their co-inhabitants were perturbed. The best approach to reveal the species interactions, therefore, is still examining the metabolic activities of each member in the community and their dynamics during co-culture, which we were not able to extend our project to, but will be performed in further study.

The effect of plasticity on community stability was still unclear from our investigations. Although linear stability analyses indicate that plasticity has supported asymptotic stability, this could be invalid if the inferred co-culture equilibria from fitted gLV models were inaccurate, which actually were demonstrated to be highly probable. Moreover, almost no effect of plasticity on species persistence was observed, since species were always able to remain in the community upon perturbation regardless of the presence of plasticity. Despite these limitations, as discussed above, the results from species persistence experiments support that most of the communities showed no dependence between members when there was plasticity, while a number of them showed competitive dependence when there was no plasticity. These suggest that plasticity could possibly support community stability by diminishing species interactions, or dependence. This was also suggested by Coyte *et al*., although their work was based on the use of the gLV model [9]. Nevertheless, it is important to develop a more comprehensive framework for assessing community stability with our mechanistic model of plastic metabolism and dynamic metabolic interactions. We believe there could be plenty of rooms for further research in this direction. Our model allows monitoring many characteristics of each species members, ranging from population density, growth rate, to metabolic activities. It is also feasible to track the nutrient dynamics of the environment. Hence, multiple facets community stability [34, 35], such as community resistance [16, 17], resilience [24], and robustness [36], both in terms of composition and function, are expected to be feasibly studied.

Overall, our study has shed light onto how adaptive plasticity could affect species coexistence and metabolic interactions, which in turn could play crucial roles in shaping the diversity and stability of microbial communities. In order to obtain a more thorough understanding of these impacts, in addition to the above suggestions, it is also necessary to extend the investigations to more species and environments such that a more diverse number of scenarios could be explored. Also importantly, the impacts should be studied at communities with larger size. This would not only enable the findings to be more biologically relevant, but also help decipher the role of higher-order interactions and the predictability of pairwise interactions, which are still controversial among studies [10, 37, 38]. Other mechanisms and/or types of interactions that also regulate the structure and function of microbial communities are also needed to be taken into consideration. These could be bacterial chemical, mechanical, or biological warfare [28, 39]; bacterial motility [29, 30, 40]; and host biology [41].

References

1. **Trivedi P**, **Leach JE**, **Tringe SG**, **Sa T**, **Singh BK**. Plant–microbiome interactions: from community assembly to plant health. *Nat Rev Microbiol 2020 1811*. 2020;18: 607–621. doi:10.1038/S41579-020-0412-1

2. **Grond K**, **Sandercock BK**, **Jumpponen A**, **Zeglin LH**. The avian gut microbiota: community, physiology and function in wild birds. *J Avian Biol*. 2018;49: e01788. doi:10.1111/jav.01788

3. **van de Guchte M**, **Blottière HM**, **Doré J**. Humans as holobionts: implications for prevention and therapy. *Microbiome*. 2018;6: 81. doi:10.1186/s40168-018-0466-8

4. **Bardgett RD**, **Freeman C**, **Ostle NJ**. Microbial contributions to climate change through carbon cycle feedbacks. ISME Journal. *ISME J*; 2008. pp. 805–814. doi:10.1038/ismej.2008.58

5. **Alvarez-Yela AC**, **Mosquera-Rendón J**, **Noreña-P A**, **Cristancho M**, **López-Alvarez D**. Microbial Diversity Exploration of Marine Hosts at Serrana Bank, a Coral Atoll of the Seaflower Biosphere Reserve. *Front Mar Sci*. 2019;0: 338. doi:10.3389/FMARS.2019.00338

6. **Fredrickson JK**, **JK F**. Ecological communities by design. *Science (80-)*. 2015;348: 1425–1427. doi:10.1126/science.aab0946

7. **Prosser JI, Bohannan BJM, Curtis TP, Ellis RJ, Firestone MK, Freckleton RP, et al.** The role of ecological theory in microbial ecology. *Nat Rev Microbiol*. 2007;5: 384–392. doi:10.1038/nrmicro1643

8. **Kumar M**, **Ji B**, **Zengler K**, **Nielsen J**. Modelling approaches for studying the microbiome. *Nat Microbiol*. 2019;4: 1253–1267. doi:10.1038/s41564-019-0491-9

9. **Coyte KZ**, **Schluter J**, **Foster KR**. The ecology of the microbiome: Networks, competition, and stability. *Science (80-)*. 2015;350: 663–666. doi:10.1126/science.aad2602

10. **Friedman J**, **Higgins LM**, **Gore J**. Community structure follows simple assembly rules in microbial microcosms. *Nat Ecol Evol*. 2017;1: 1–7. doi:10.1038/s41559-017-0109

11. **Coyte KZ**, **Rao C**, **Rakoff-Nahoum S**, **Foster KR**. Ecological rules for the assembly of microbiome communities. Gordo I, editor. *PLOS Biol*. 2021;19: e3001116. doi:10.1371/journal.pbio.3001116

12. **Rao C**, **Coyte KZ**, **Bainter W**, **Geha RS**, **Martin CR**, **Rakoff-Nahoum S**. Multi-kingdom ecological drivers of microbiota assembly in preterm infants. *Nature*. 2021;591: 633–638. doi:10.1038/s41586-021-03241-8

13. **Stein RR, Bucci V, Toussaint NC, Buffie CG, Rätsch G, Pamer EG, et al.** Ecological Modeling from Time-Series Inference: Insight into Dynamics and Stability of Intestinal

Microbiota. *PLOS Comput Biol*. 2013;9: e1003388. doi:10.1371/JOURNAL.PCBI.1003388

14. **Lax S**, **Abreu CI**, **Gore J**. Higher temperatures generically favour slower-growing bacterial species in multispecies communities. *Nat Ecol Evol 2020 44*. 2020;4: 560–567. doi:10.1038/S41559-020-1126-5

15. **Braga RM**, **Dourado MN**, **Araújo WL**. Microbial interactions: ecology in a molecular perspective. *Brazilian J Microbiol*. 2016;47: 86–98. doi:10.1016/J.BJM.2016.10.005

16. **Allison SD**, **Martiny JBH**. Resistance, resilience, and redundancy in microbial communities. *Proc Natl Acad Sci U S A*. 2008;105: 11512. doi:10.1073/PNAS.0801925105

17. **Comte J**, **Fauteux L**, **Giorgio PA del**. Links between metabolic plasticity and functional redundancy in freshwater bacterioplankton communities. *Front Microbiol*. 2013;4. doi:10.3389/FMICB.2013.00112

18. **Beier S**, **Rivers AR**, **Moran MA**, **Obernosterer I**. Phenotypic plasticity in heterotrophic marine microbial communities in continuous cultures. *ISME J 2015 95*. 2014;9: 1141–1151. doi:10.1038/ISMEJ.2014.206

19. **Brunner JD**, **Chia N**. Metabolite-mediated modelling of microbial community dynamics captures emergent behaviour more effectively than species–species modelling. *J R Soc Interface*. 2019;16. doi:10.1098/RSIF.2019.0423

20. **Pacciani-Mori L**, **Giometto A**, **Suweis S**, **Maritan A**. Dynamic metabolic adaptation can promote species coexistence in competitive microbial communities. *PLoS Comput Biol*. 2020;16. doi:10.1371/journal.pcbi.1007896

21. **Oña L**, **Kost C**. Cooperation increases robustness to ecological disturbance in microbial cross-feeding networks. *bioRxiv*. 2020; 2020.05.15.098103. doi:10.1101/2020.05.15.098103

22. **Magnúsdóttir S, Heinken A, Kutt L, Ravcheev DA, Bauer E, Noronha A, et al.** Generation of genome-scale metabolic reconstructions for 773 members of the human gut microbiota. *Nat Biotechnol*. 2017;35: 81–89. doi:10.1038/nbt.3703

23. **Bornstein BJ**, **Keating SM**, **Jouraku A**, **Hucka M**. LibSBML: An API Library for SBML. *Bioinformatics*. 2008;24: 880. doi:10.1093/BIOINFORMATICS/BTN051

24. **Haydon D**. Pivotal Assumptions Determining the Relationship between Stability and Complexity: An Analytical Synthesis of the Stability-Complexity Debate. *https://doi.org/101086/285658*. 2015;144: 14–29. doi:10.1086/285658

25. **Harris CR, Millman KJ, Walt SJ van der, Gommers R, Virtanen P, Cournapeau D, et al.** Array programming with NumPy. *Nat 2020 5857825*. 2020;585: 357–362. doi:10.1038/s41586-020-2649-2

26. **Virtanen P, Gommers R, Oliphant TE, Haberland M, Reddy T, Cournapeau D, et al.** SciPy 1.0: fundamental algorithms for scientific computing in Python. *Nat Methods 2020 173*. 2020;17: 261–272. doi:10.1038/s41592-019-0686-2

27. **Waskom M, Botvinnik O, O'Kane D, Hobson P, Ostblom J, Lukauskas S, et al.** mwaskom/seaborn: v0.9.0 (July 2018). 16 Jul 2018 [cited 20 Jun 2019]. doi:10.5281/ZENODO.1313201

28. **Granato ET**, **Meiller-Legrand TA**, **Foster KR**. The Evolution and Ecology of Bacterial Warfare. *Curr Biol*. 2019;29: R521–R537. doi:10.1016/j.cub.2019.04.024

29. **Kennedy MJ**. Role of Motility, Chemotaxis, and Adhesion in Microbial Ecology. *Ann N Y Acad Sci*. 1987;506: 260–273. doi:10.1111/j.1749-6632.1987.tb23825.x

30. **Neville BA, Forde BM, Claesson MJ, Darby T, Coghlan A, Nally K, et al.** Characterization of Pro-Inflammatory Flagellin Proteins Produced by Lactobacillus ruminis and Related Motile Lactobacilli. *PLoS One*. 2012;7: e40592. doi:10.1371/JOURNAL.PONE.0040592

31. **Mounier J, Monnet C, Vallaeys T, Arditi R, Sarthou A-S, Hélias A, et al.** Microbial Interactions within a Cheese Microbial Community. *Appl Environ Microbiol*. 2008;74: 172. doi:10.1128/AEM.01338-07

32. **Venturelli OS, Carr A V, Fisher G, Hsu RH, Lau R, Bowen BP, et al.** Deciphering microbial interactions in synthetic human gut microbiome communities. *Mol Syst Biol*. 2018;14: e8157. doi:10.15252/msb.20178157

33. **Costa JCCP**, **Bolívar A**, **Valero A**, **Carrasco E**, **Zurera G**, **Pérez-Rodríguez F**. Evaluation of the effect of Lactobacillus sakei strain L115 on Listeria monocytogenes at different conditions of temperature by using predictive interaction models. *Food Res Int*. 2020;131. doi:10.1016/j.foodres.2019.108928

34. **Donohue I, Hillebrand H, Montoya JM, Petchey OL, Pimm SL, Fowler MS, et al.** Navigating the complexity of ecological stability. *Ecol Lett*. 2016;19: 1172–1185. doi:10.1111/ELE.12648

35. **Landi P**, **Minoarivelo HO**, **Brännström Å**, **Hui C**, **Dieckmann U**. Complexity and stability of ecological networks: a review of the theory. *Popul Ecol*. 2018;60: 319–345. doi:10.1007/s10144-018-0628-3

36. **Levin SA**, **Lubchenco J**. Resilience, Robustness, and Marine Ecosystem-based Management. *Bioscience*. 2008;58: 27–32. doi:10.1641/B580107

37. **Momeni B**, **Xie L**, **Shou W**. Lotka-Volterra pairwise modeling fails to capture diverse pairwise microbial interactions. *Elife*. 2017;6. doi:10.7554/eLife.25051.001

38. **Sanchez-Gorostiaga A**, **Bajić D**, **Osborne ML**, **Poyatos JF**, **Sanchez A**. High-order interactions distort the functional landscape of microbial consortia. *PLoS Biol*. 2019;17: e3000550. doi:10.1371/journal.pbio.3000550

39. **Czárán TL**, **Hoekstra RF**, **Pagie L**. Chemical warfare between microbes promotes biodiversity. *Proc Natl Acad Sci*. 2002;99: 786–790. doi:10.1073/PNAS.012399899

40. **Gude S**, **Pinçe E**, **Taute KM**, **Seinen AB**, **Shimizu TS**, **Tans SJ**. Bacterial coexistence driven by motility and spatial competition. *Nature*. 2020;578: 588–592. doi:10.1038/s41586-020-2033-2

41. **Foster KR**, **Schluter J**, **Coyte KZ**, **Rakoff-Nahoum S**. The evolution of the host microbiome as an ecosystem on a leash. *Nature*. 2017;548: 43–51. doi:10.1038/nature23292

Appendices

Table S1: List of species whose genome-scale metabolic network used in the study. The reconstructed metabolic networks were collected from AGORA database v.1.3. Bold text indicates species selected for co-culture experiments.

Species ID	Strain name	Phylum	Class	Gram staining
setA_9	Corynebacterium_ulcerans_809	Actinobacteria	Actinobacteria	+
setA_18	Microbacterium_oleivorans_NBRC_103075	Actinobacteria	Actinobacteria	+
setA_11	**Eggerthella_lenta_DSM_2243**	**Actinobacteria**	**Coriobacteriia**	**+**
setA_3	Alistipes_finegoldii_DSM_17242	Bacteroidetes	Bacteroidia	-
setA_4	Bacteroides_caccae_ATCC_43185	Bacteroidetes	Bacteroidia	-
setA_19	Odoribacter_laneus_YIT_12061	Bacteroidetes	Bacteroidia	-
setA_22	Prevotella_ruminicola_23	Bacteroidetes	Bacteroidia	-
setA_6	Brevibacillus_brevis_NBRC_100599	Firmicutes	Bacilli	+
setA_16	**Lactobacillus_gastricus_PS3**	**Firmicutes**	**Bacilli**	**+**
setA_8	Clostridium_difficile_NAP07	Firmicutes	Clostridia	+
setA_14	Faecalibacterium_cf_prausnitzii_KLE1255	Firmicutes	Clostridia	+
setA_24	**Ruminococcus_lactaris_ATCC_29176**	**Firmicutes**	**Clostridia**	**+**
setA_20	Peptoniphilus_timonensis_JC401	Firmicutes	Tissierellia	+
setA_17	Methyloversatilis_universalis_Fam50001	Proteobacteria	Beta	-
setA_15	**Helicobacter_pylori_26695**	**Proteobacteria**	**Epsilon**	**-**
setA_13	Escherichia_coli_str_K_12_substr_MG1655	Proteobacteria	Gamma	-
setA_21	**Pseudomonas_nitroreducens_HBP1**	**Proteobacteria**	**Gamma**	**-**
setA_26	Vibrio_mimicus_MB_451	Proteobacteria	Gamma	+

Figure S1 (page 31): Population densities at equilibrium (ρ, measured by densities the end of simulations – see Methods) in batch mono-culture. Yellow points and violin plots illustrate the distributions of multiple densities ρ_{ON} (ρ when plasticity=ON) resulted from 10 replicates. The distributions are not represented by violin plots when standard deviation of $\rho_{ON} \leq 0.1$. Yellow horizontal lines represent the means of ρ_{ON}. Greyish blue lines represent ρ_{OFF} (ρ when plasticity=OFF), which have no stochasticity and take single value for every species-environment case. Representative cases in Fig. 1A were extracted from here.

Figure S2 (page 32): Population densities at equilibrium (ρ, measured by densities the end of simulations – see Methods) in continuous mono-culture. Yellow points and violin plots illustrate the distributions of multiple densities ρ_{ON} (ρ when plasticity=ON) resulted from 10 replicates. The distributions are not represented by violin plots when standard deviation of $\rho_{ON} \leq 0.1$. Yellow horizontal lines represent the means of ρ_{ON}. Greyish blue lines represent ρ_{OFF} (ρ when plasticity=OFF), which have no stochasticity and take single value for every species-environment case. Representative cases in Fig. 1B were extracted from here.

Figure S3: Heatmaps illustrating intrinsic plasticity values (P_{mono}) across all studied species (n=18) in all tested media (n=11) in batch (left) and continuous (right) culture. Dendrograms represent hierarchical clustering of species (vertical) or of media (horizontal) based on the intrinsic plasticity profiles. Species are annotated for their taxonomy at phylum and class levels by the two leftmost columns (see Key). By the two uppermost rows, media are, sequentially, annotated for their ranked Shannon nutrient diversity (H, see Key) and their associated principal clusters resulted from hierarchical clustering on nutrient concentration profiles (see Key and Fig. 3).

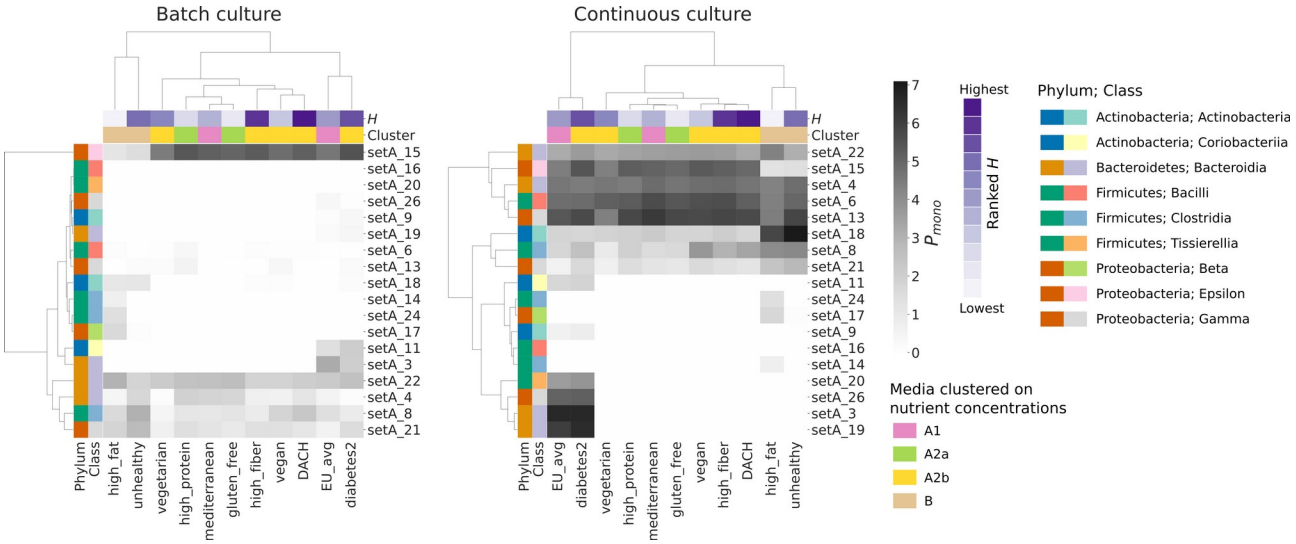

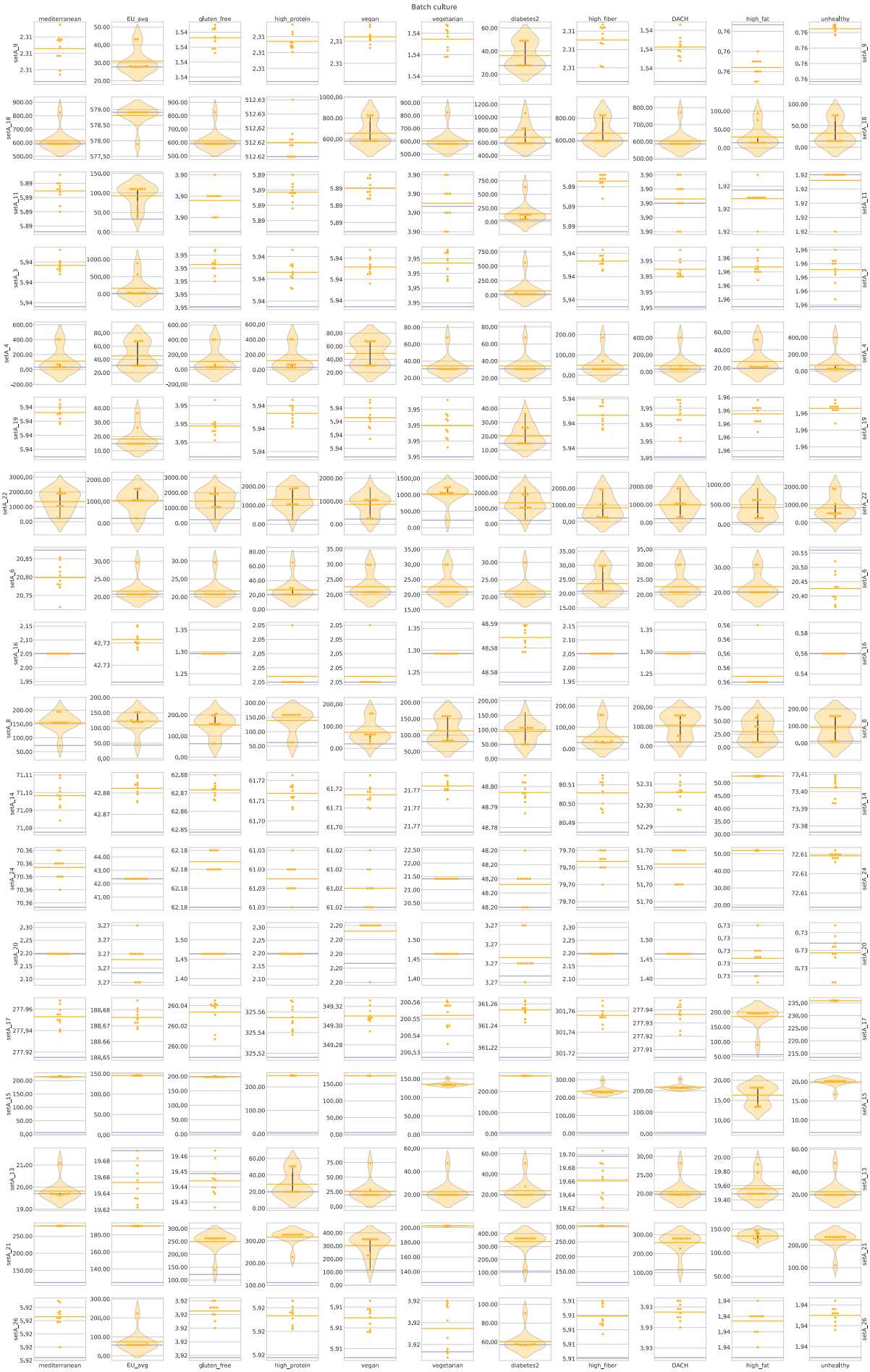
Batch culture
mediterranean
EU_avg
gluten_free
high_protein
vegan
vegetarian
diabetes2
high_fiber
DACH
high_fat
unhealthy
setA_9
setA_18
setA_11
setA_3
setA_4
setA_19
setA_22
setA_6
setA_16
setA_8
setA_14
setA_24
setA_20
setA_17
setA_15
setA_13
setA_21
setA_26

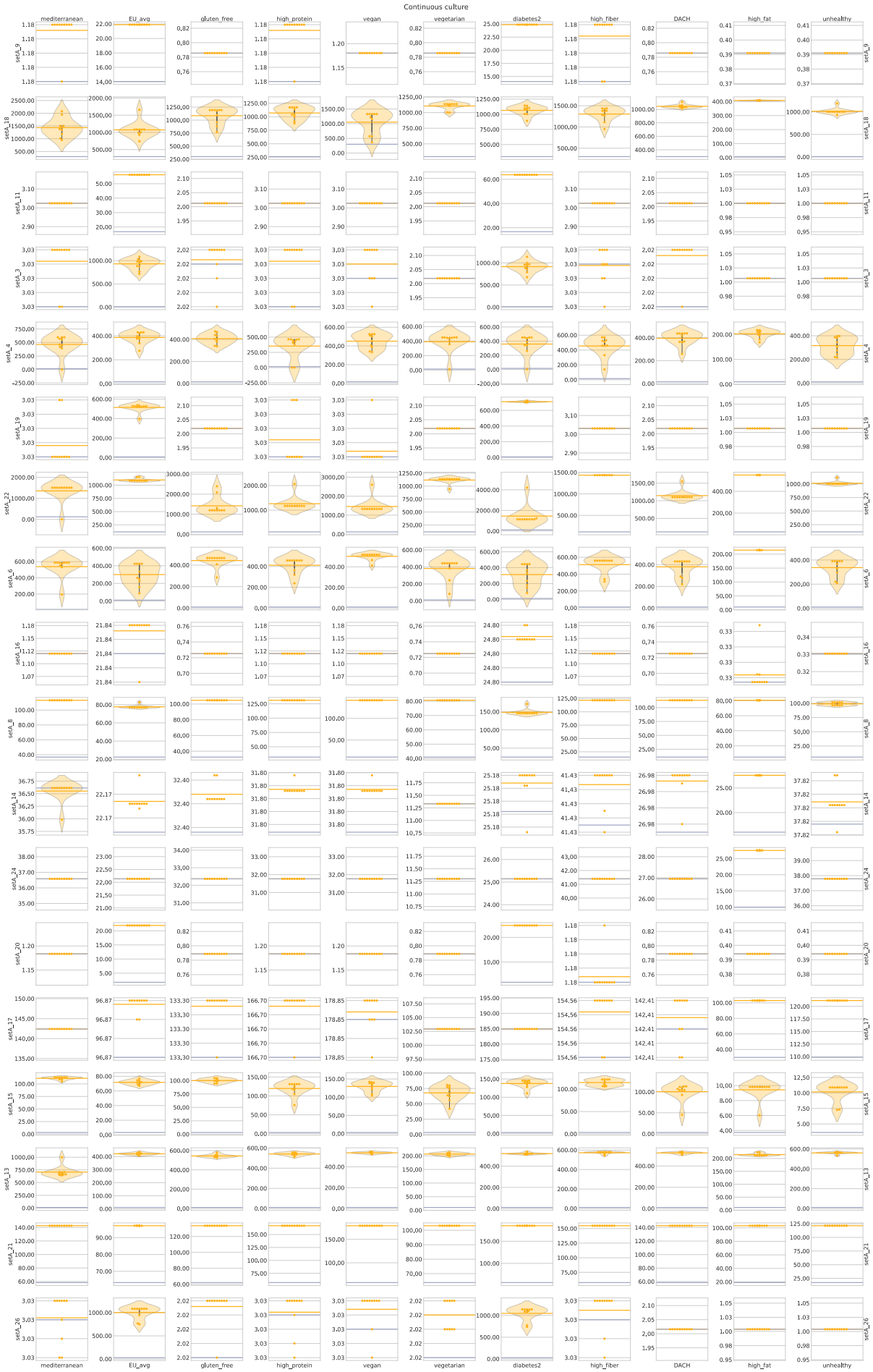
Continuous culture
mediterranean
EU_avg
gluten_free
high_protein
vegan
vegetarian
diabetes2
high_fiber
DACH
high_fat
unhealthy
setA_9
setA_18
setA_11
setA_3
setA_4
setA_19
setA_22
setA_6
setA_16
setA_8
setA_14
setA_24
setA_20
setA_17
setA_15
setA_13
setA_21
setA_26

Figure S4 (page 34): Population densities at equilibrium (ρ, measured by densities the end of simulations – see Methods) in batch mono- and co-culture in *EU_avg* (A) and *high_fat* (B) media. Elements in purple are from mono-culture experiments, while elements in green are from co-culture experiments. Points and violin plots illustrate the distributions of multiple densities ρ_{ON} (ρ when plasticity=ON) resulted from 10 replicates. The distributions are not represented by violin plots when standard deviation of $\rho_{ON} \leq 0.1$. Bold horizontal lines represent the means of ρ_{ON}. Dashed horizontal lines represent ρ_{OFF} (ρ when plasticity=OFF), which have no stochasticity and take single value for every case.

Figure S5 (page 35): Population densities at equilibrium (ρ, measured by densities the end of simulations – see Methods) in continuous mono- and co-culture in *EU_avg* (A) and *high_fat* (B) media. Elements in purple are from mono-culture experiments, while elements in green are from co-culture experiments. Points and violin plots illustrate the distributions of multiple densities ρ_{ON} (ρ when plasticity=ON) resulted from 10 replicates. The distributions are not represented by violin plots when standard deviation of $\rho_{ON} \leq 0.1$. Bold horizontal lines represent the means of ρ_{ON}. Dashed horizontal lines represent ρ_{OFF} (ρ when plasticity=OFF), which have no stochasticity and take single value for every case.

Figure S6: The effect of plasticity on growth of member species in continuous co-culture supplemented with *EU_avg* (left) and *high_fat* (right) media, measured as P_{co} (see Methods). In each heatmap, an off-diagonal cell displays the P_{co} value of species in the corresponding row when it was co-cultured with species in the corresponding column. At each heatmap, the left-hand column corresponds to the intrinsic plasticity (P_{mono}) values of the species.

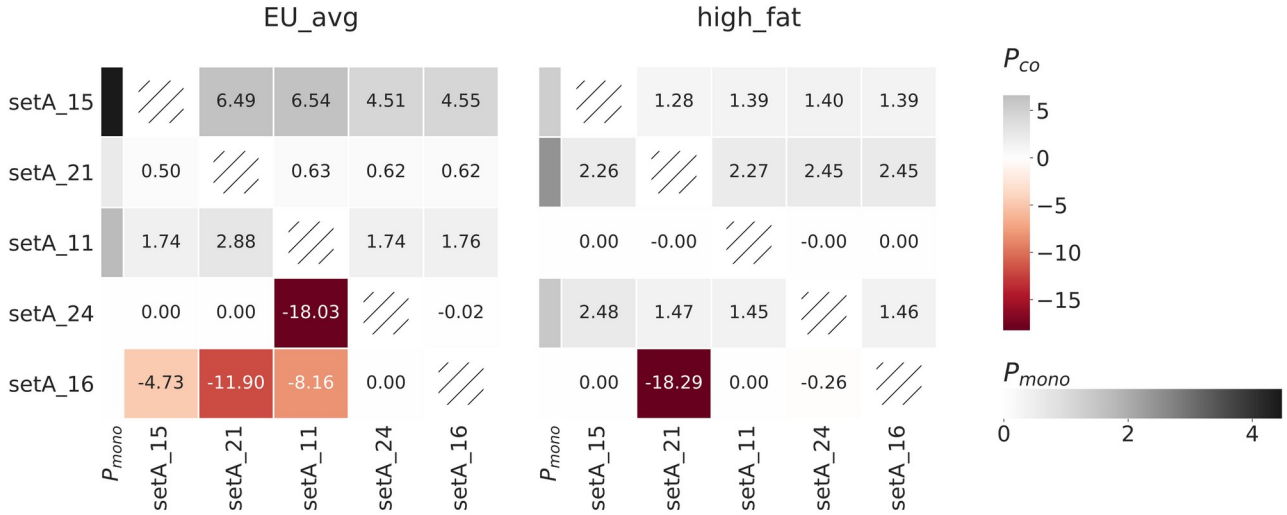

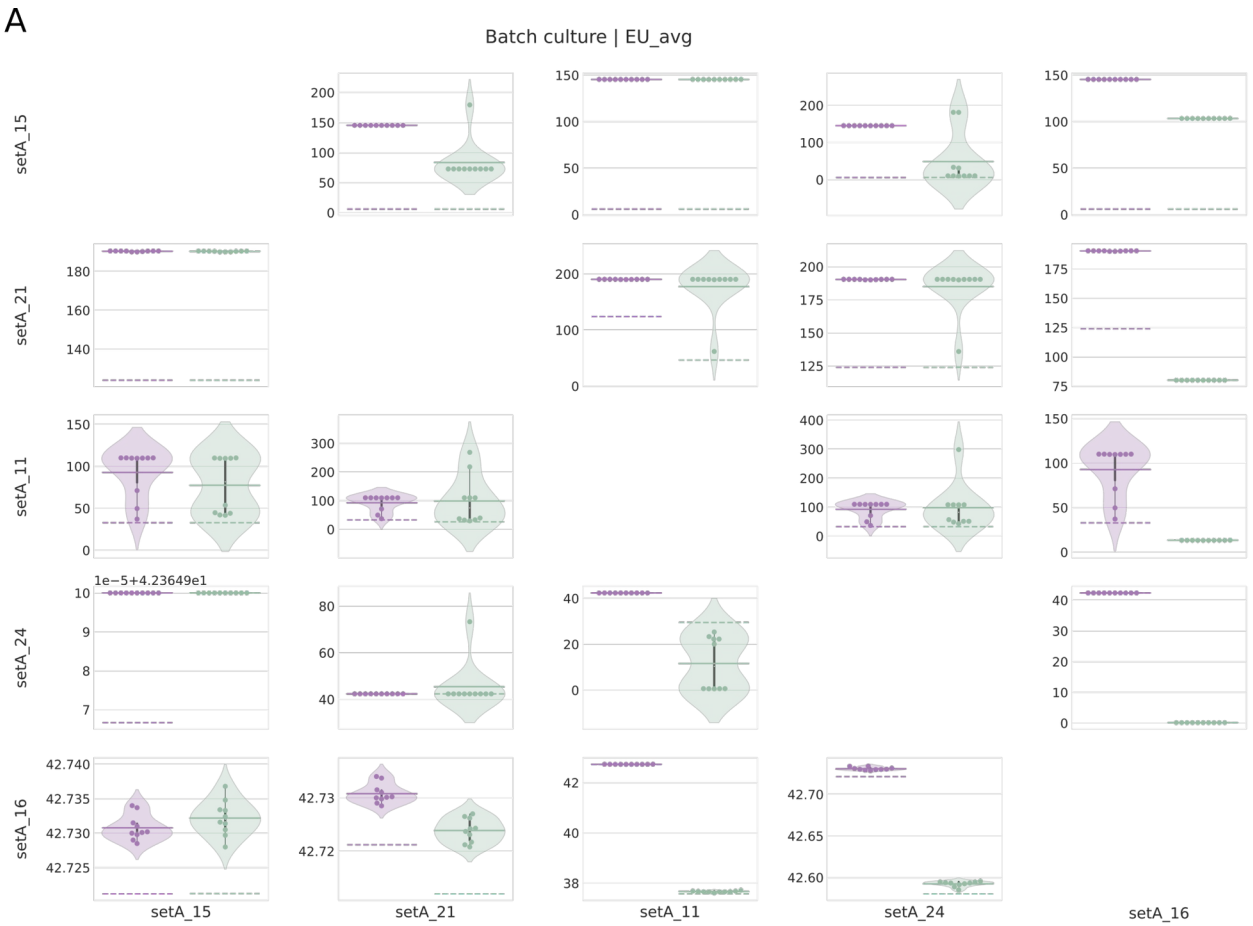
A
Batch culture | EU_avg
setA_15
setA_21
setA_11
setA_24
setA_16
1e−5+4.23649e1
setA_15
setA_21
setA_11
setA_24
setA_16

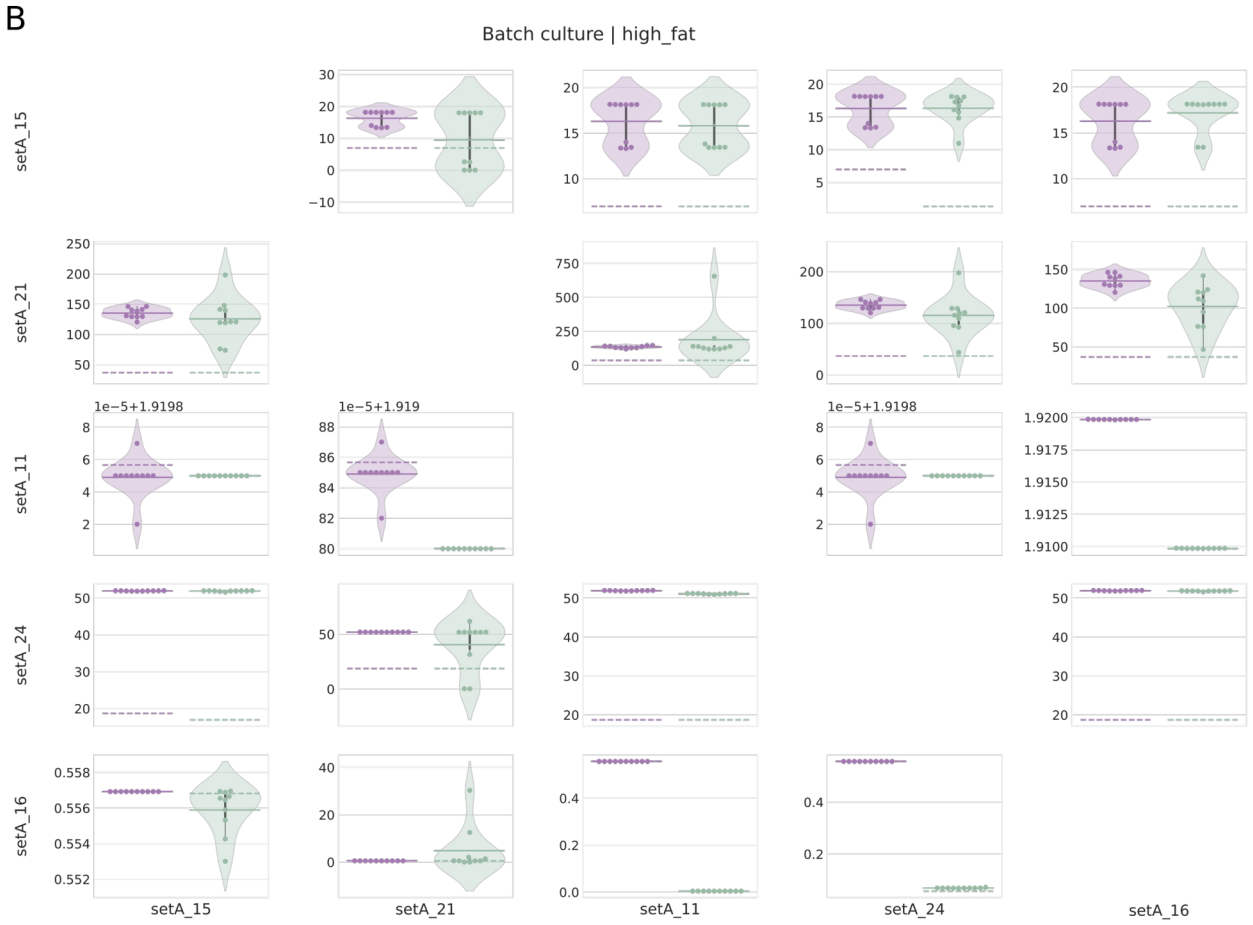
B
Batch culture | high_fat
setA_15
setA_21
setA_11
setA_24
setA_16
1e−5+1.9198
1e−5+1.919
1e−5+1.9198
setA_15
setA_21
setA_11
setA_24
setA_16

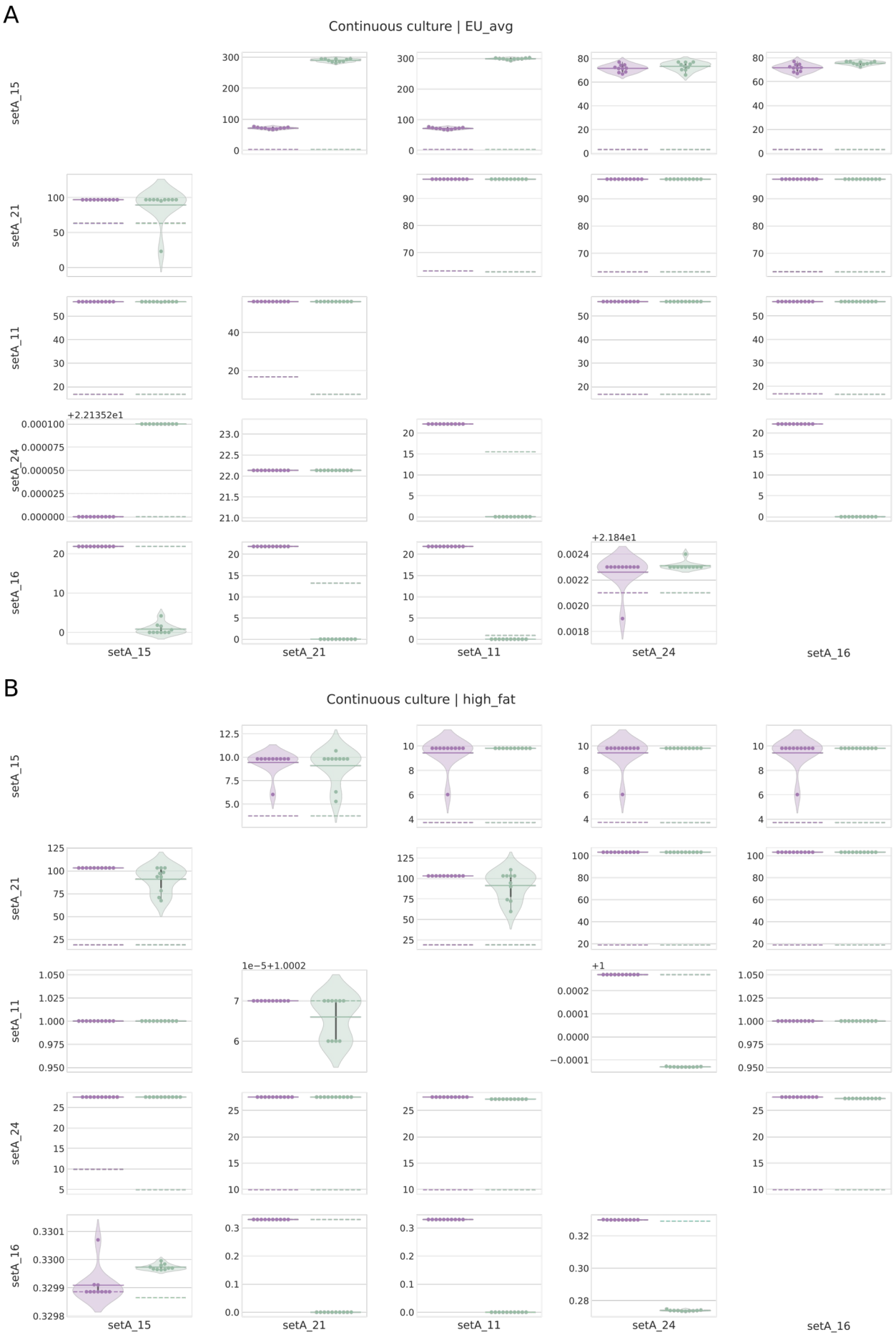
A
Continuous culture | EU_avg
setA_15
setA_21
setA_11
setA_24
setA_16
+2.21352e1
+2.184e1
B
Continuous culture | high_fat
1e−5+1.0002
+1

Figure S7: Species interactions in continuous co-culture simulations with plasticity=OFF and with plasticity=ON in *EU_avg* (A-C) and *high_fat* (B-D) media. In each heatmap, an off-diagonal cell displays the value of species in the corresponding row when it was co-cultured with species in the corresponding column. (A-B) The heatmaps illustrate competitive exclusion measurements only. Positive values indicate the superior members while negative values indicate the inferior members. The corresponding absolute values are the proportions of replicates with competitive exclusion events indicated (see Key). (C-D) The heatmaps illustrate species interaction coefficients overlaid with competitive exclusion measurements. Cells on the leading diagonal represent intra-species interaction coefficients. Inter-species interaction coefficients were inferred only if a simulation indicated to not experience a competitive exclusion event. The coefficient represented by an off-diagonal cell indicates the effect of species in the associated column on species in the associated row, which can be positive, negative, or neutral (+/-/0). At a community which was indicated with competitive exclusion in only a part of its replicates, competitive exclusion measurements are displayed by smaller squares, nested inside cells displaying species interaction coefficients. In each (A), (B), (C), and (D), the leftmost column corresponds to the intrinsic plasticity (P_{mono}) values of the species.

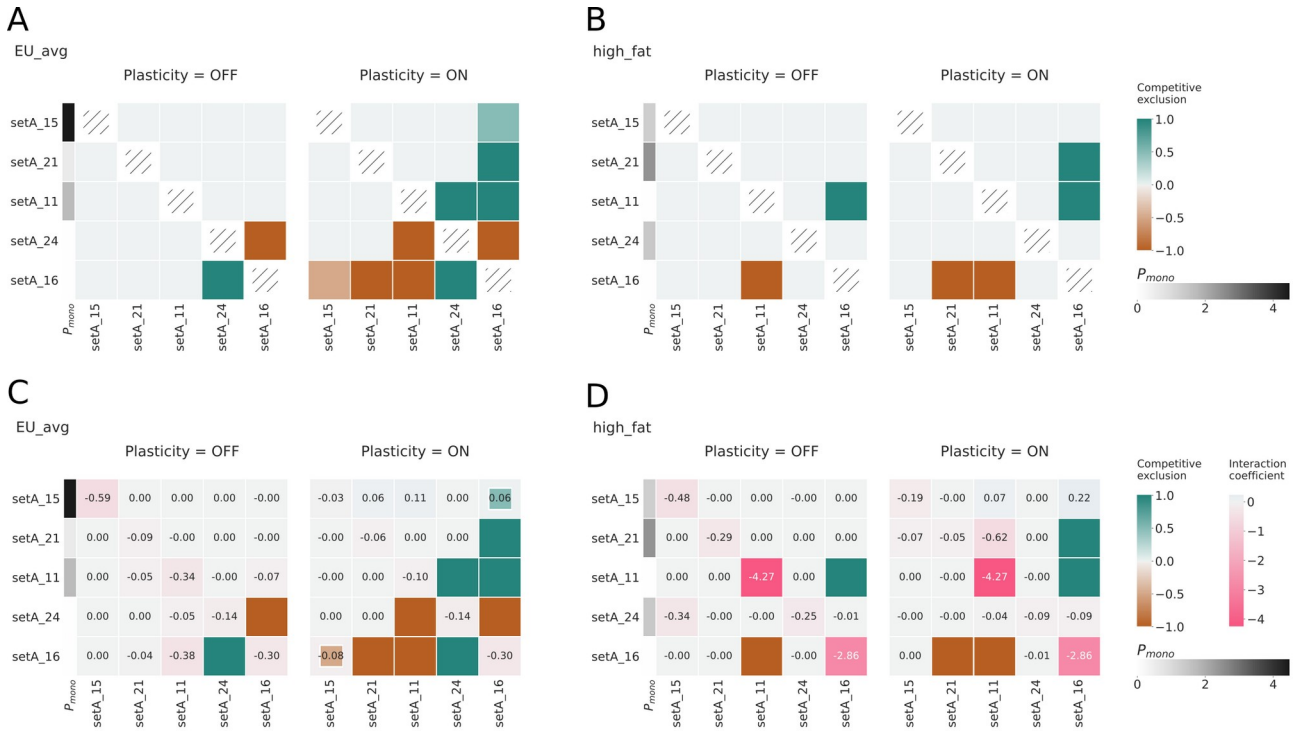

Figure S8 (page 37-38): Plots of species density over time in co-culture simulations with pulse perturbations when plasticity=OFF (left panel) and when plasticity=ON (right panel) in *high_fat* medium. Thin vertical blocks in grey highlight the period that the perturbations occurred (duration of 1 hour). Yellow lightning bolts indicate species members which the introduced perturbations targeted to. When plasticity=ON, multiple curves in different colours represent results from different 10 replicates. Experiments with perturbations were not conducted on simulations indicated to experience competitive exclusion.

Plasticity=OFF

Plasticity=ON

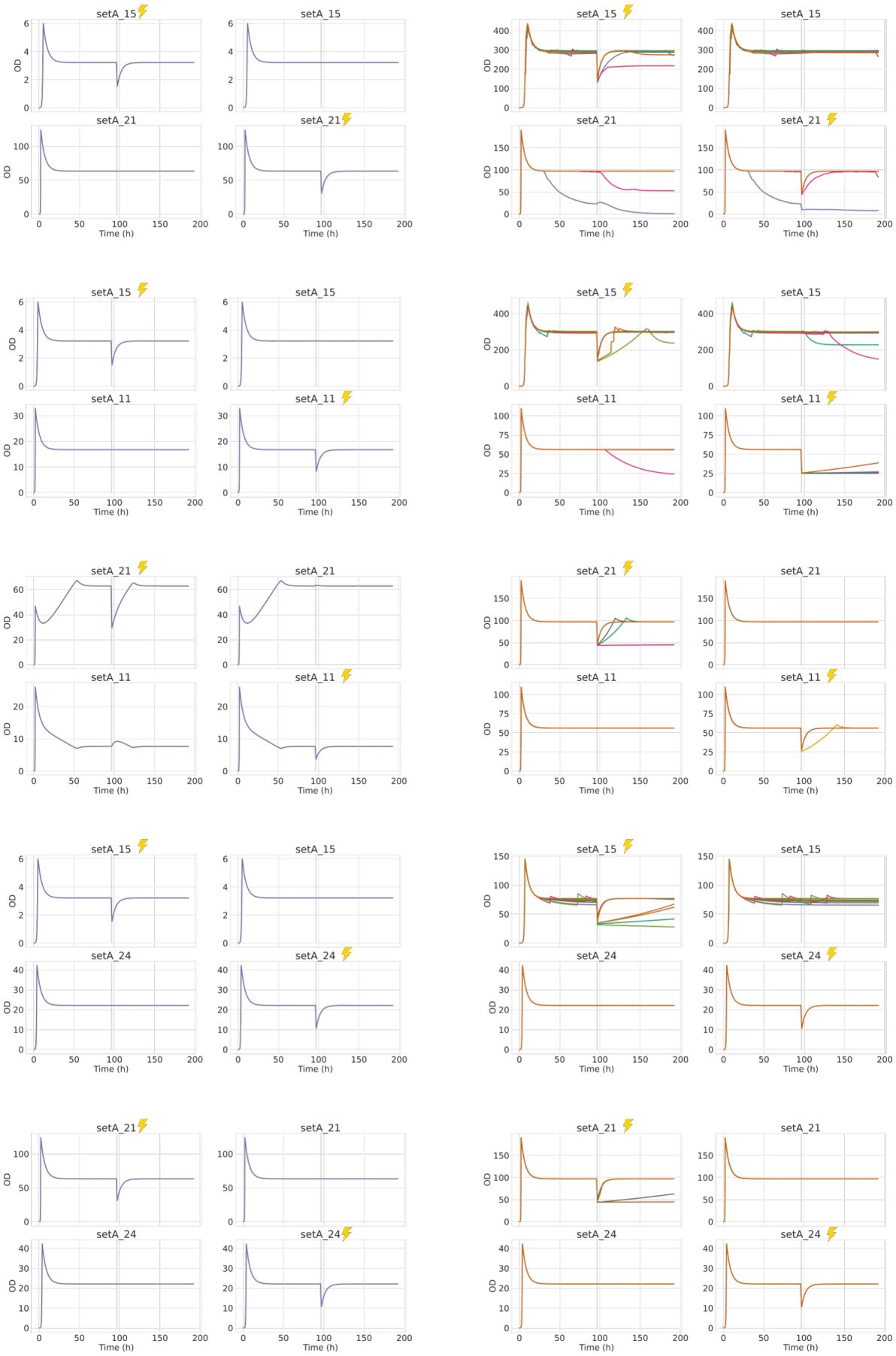

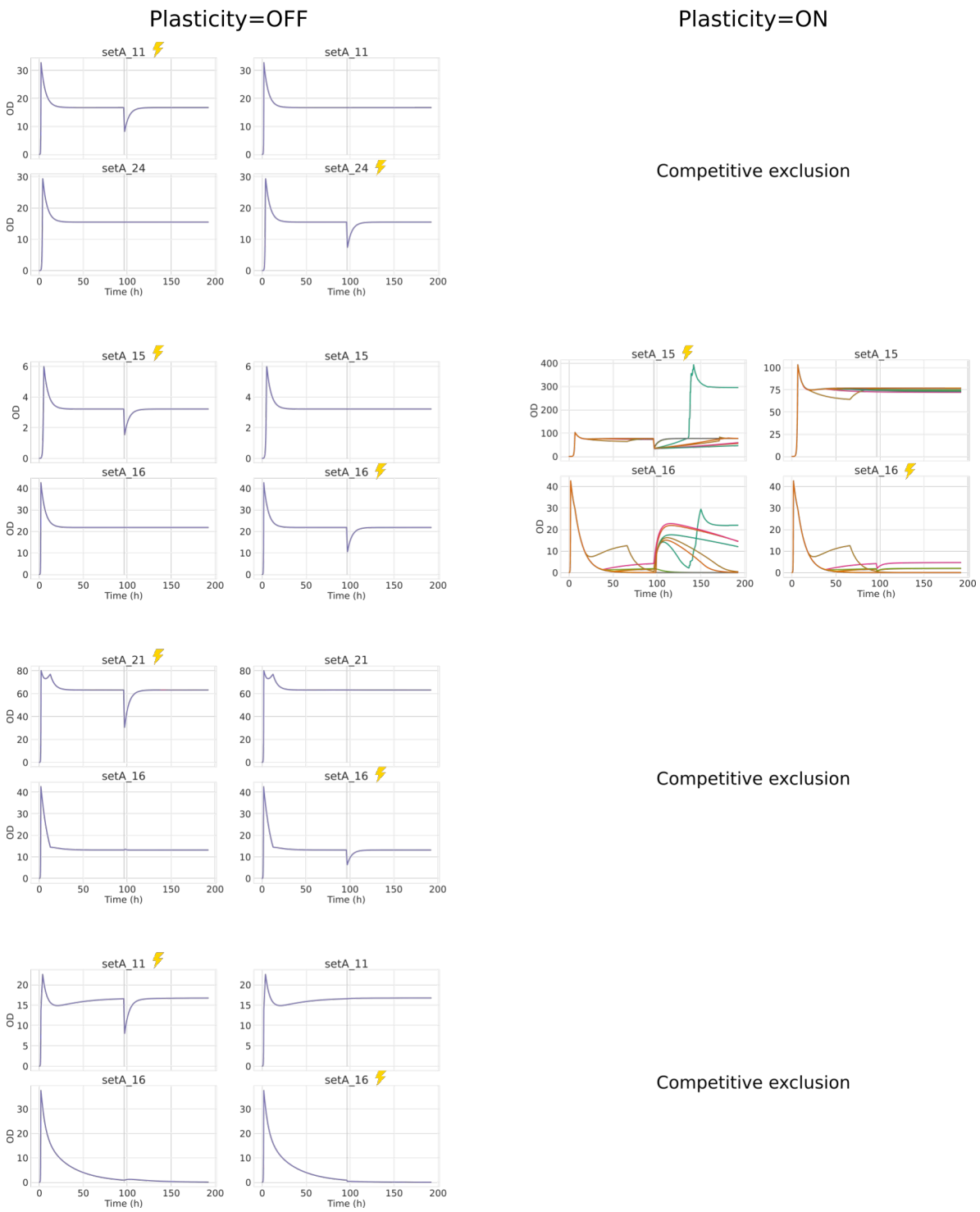

Figure S9 (page 39-40): Plots of species density over time in co-culture simulations with pulse perturbations when plasticity=OFF (left panel) and when plasticity=ON (right panel) in *high_fat* medium. Thin vertical blocks in grey highlight the period that the perturbations occurred (duration of 1 hour). Yellow lightning bolts indicate species members which the introduced perturbations targeted to. When plasticity=ON, multiple curves in different colours represent results from different 10 replicates. Experiments with perturbations were not conducted on simulations indicated to experience competitive exclusion.

Plasticity=OFF

Plasticity=ON

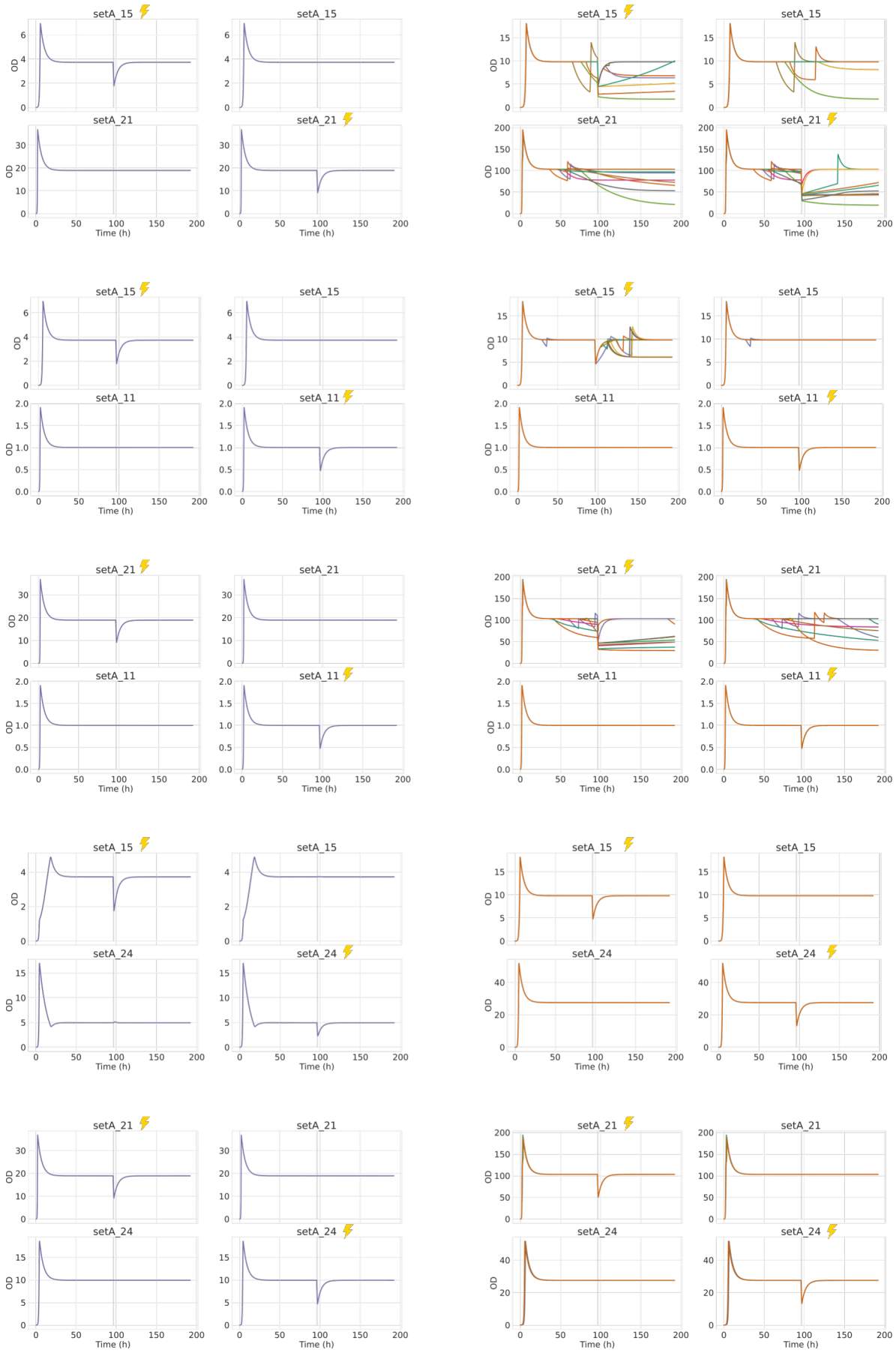

Plasticity=OFF

Plasticity=ON

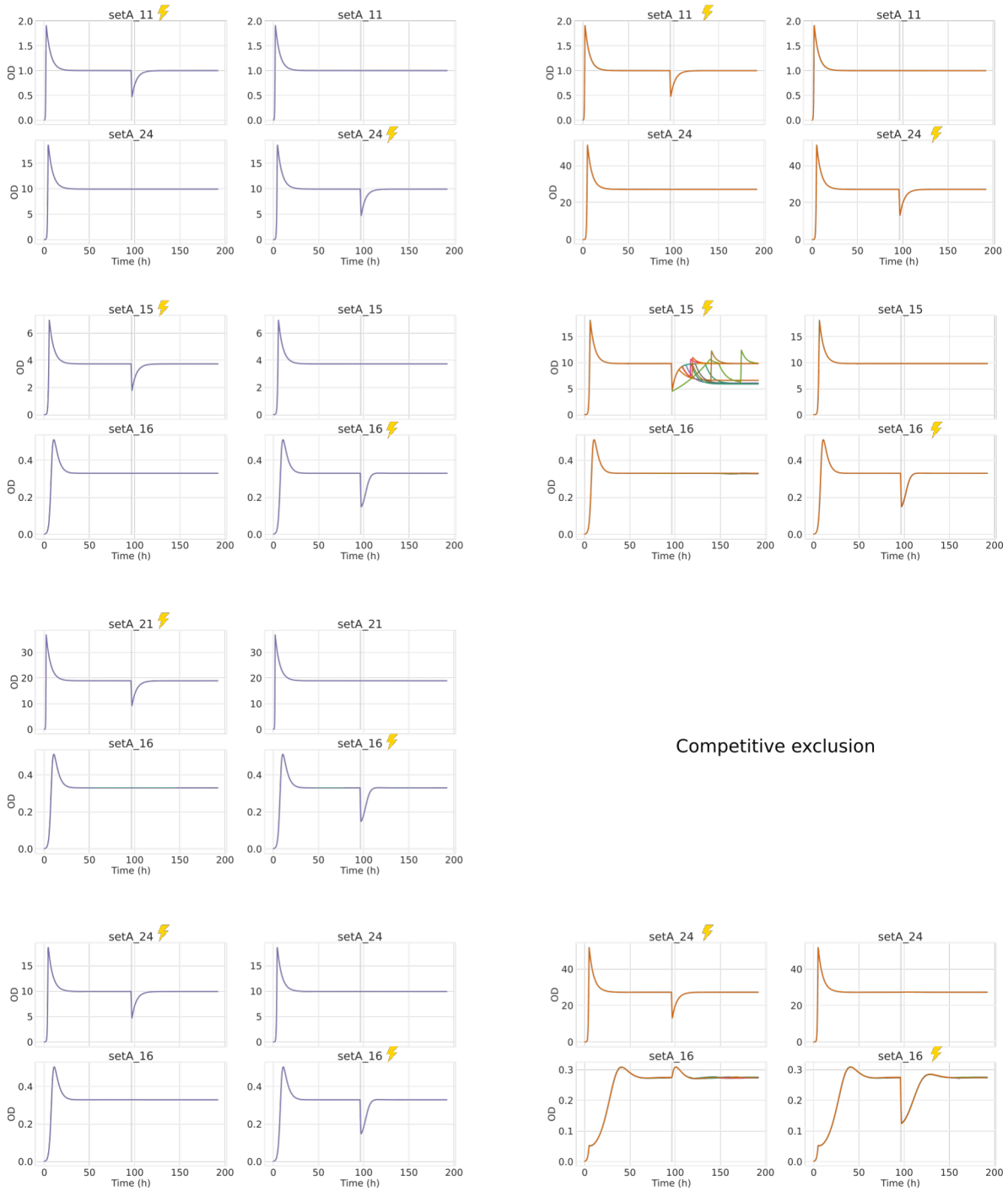

Competitive exclusion